

Automatic Lesion Detection System (ALDS) for Skin Cancer Classification Using SVM and Neural Classifiers

By

Muhammad Ali Farooq

NUST201463693MPNEC45014F



PAKISTAN NAVY ENGINEERING COLLEGE, PNS JAUHAR,
KARACHI

NATIONAL UNIVERSITY OF SCIENCES AND TECHNOLOGY,
ISLAMABAD

April 10, 2017

**Automatic Lesion Detection System (ALDS) for Skin Cancer Classification
Using SVM and Neural Classifiers**

By

Muhammad Ali Farooq

NUST201463693MPNEC45014F



Supervised by

Dr. Rana Hammad Raza

A dissertation submitted to

PAKISTAN NAVY ENGINEERING COLLEGE
NATIONAL UNIVERSITY OF SCIENCES AND TECHNOLOGY, ISLAMABAD

A thesis submitted in fulfillment of the requirements

For the degree of Master Program

in the

Electrical Engineering (Control)

Department of Electronic and Power Engineering (EPE)

April 10, 2017

National University of Sciences and Technology

MASTER'S THESIS WORK

We hereby recommend that the dissertation prepared under our supervision by:
(Student Name & Regn No.) Muhammad Ali Farooq (NUST201463693MPNEC45014F)
Titled: Automatic Lesion Detection System (ALDS) for Skin Cancer Classification Using SVM and Neural Classifiers be accepted in partial fulfillment of the requirements for the award of Master's Degree.

Examination Committee Members

1. Name: Dr Ali Hanzalah Khan Signature: _____

2. Name: Dr Adeel Yusuf Signature: _____

Supervisor's name: Dr Rana Hammad Raza Signature: _____

Date: _____

Head of Department

Date

COUNTERSIGNED

Date: _____

Dean / Principal

Abstract

Technology aided platforms provide reliable tools in almost every field these days. These tools being supported by computational power are significant for applications that need sensitive and precise data analysis. One such important application in the medical field is Automatic Lesion Detection System (ALDS) for skin cancer classification. Computer aided diagnosis helps physicians and dermatologists to obtain a “second opinion” for proper analysis and treatment of skin cancer. Precise segmentation of the cancerous mole along with surrounding area is essential for proper analysis and diagnosis. This thesis is focused towards the development of improved ALDS framework based on probabilistic approach that initially utilizes active contours and watershed merged mask for segmenting out the mole and later SVM and Neural Classifier are applied for the classification of the segmented mole. After lesion segmentation, the selected features are classified to ascertain that whether the case under consideration is melanoma or non-melanoma. The approach is tested for varying datasets and comparative analysis is performed that reflects the effectiveness of the proposed system.

The second phase of proposed research work incorporate deep learning methodologies that plays an imperative role in accurate, precise and robust classification of the lesion mole. It has been reflected in the proposed work by using state of the art deep learning frameworks which includes Tensorflow and NVIDIA DIGITS for different datasets. The accuracy level using TensorFlow and NVIDIA DIGITS is 83.4 % and 81.2 % respectively. The results obtained reflects that accuracy level is better than conventional neural classifiers.

Acknowledgment

All the thanks to ALLAH Almighty (SWT) who gave the courage and knowledge to undertake this thesis work. I would like to express my deepest gratitude and thanks to my supervisor Cdr Dr Rana Hammad Raza. He patiently guided me through the course of my study program. Without his help, encouragement and motivation, this thesis work and research would not been possible. I will never forget your encouragements and continuous support during my skin cancer research work and research paper preparation. I also thank my GEC committee members Dr Adeel Yusuf and Dr Ali Hanzalah Khan for guiding me, sharing their knowledge and giving me valuable feedback throughout my thesis.

Secondly I would like to thanks my parents, and brother, for being all the way with me and without their continues support, love this thesis work and research would not been possible

Lastly I would like to acknowledge the University of Heidelberg and University of Erlangen the contributors of DermIS dataset, Galderma S.A for DermQuest and PH² database contributors for providing the image resources to carry out this research work.

Contents

Abstract	4
Acknowledgment	5
List of Abbreviations	9
List of Tables	10
List of Figures	11
Chapter 1 Introduction	14
1.1 Problem Statement	14
1.2 Thesis Structure	15
Chapter 2 Background	16
2.1 Human Skin Biology.....	16
2.1.1 Human Skin Layers.....	16
2.1.2 Types of skin moles.....	17
2.2 Skin Cancer.....	18
2.2.1 Types of skin cancer.....	18
2.2.2 Skin Cancer Facts and Statistics.....	20
2.2.3 Skin Cancer Treatments	21
2.2.4 Prevention from Skin Cancer	22
2.3 Dermoscopy	22
2.3.1 Digital Dermoscopy	23
2.4 Clinical Diagnosis Techniques	24
2.4.1 CASH Rule.....	24
2.4.2 Seven Point Checklist Method	24
2.4.3 Menzies Method.....	24
2.4.4 ABCD Method	25
2.5 Computer Aided diagnosis (CAD) Systems	26
2.5.1 Lung Nodule Detection and Chest Radiography.....	27
2.5.2 Intracranial Aneurysms Detection in MRA	27
2.5.3 Interval Changes Detection in Whole Body Scans	27
2.6 Computer Aided diagnosis (CAD) Systems for Skin Cancer Detection and Classification...	28
2.6.1 SolarScan.....	28

2.6.2 MoleMax	28
2.6.3.MelaFind	29
2.6.4 SIAscope	29
2.7 Comparison of Computer Aided diagnosis (CAD) Systems for Skin Cancer Detection and Classification	29
2.8 Proposed Computer Aided diagnosis (CAD) Systems for Skin Cancer Detection and Classification	30
Chapter 3 Skin Lesion Segmentation Using Various Techniques	32
3.1 Automatic Lesion Detection / Segmentation Methods	32
3.1.1 Preprocessing of digital dermoscopic images	32
3.1.2 Edge Detection Methods	33
3.1.2.1 Prewitt and Sobel Edge Detector.....	33
3.1.2.2 Canny Edge Detector.....	34
3.1.3 Region Based Segmentation Techniques	35
3.1.4 Active Contours Method	36
3.1.5 Watershed Segmentation	37
3.2 Advanced Segmentation Approaches	39
Chapter 4 Skin Cancer Feature Vectors and Classifiers Using Various Machine Learning Methods.....	40
4.1 Feature Vectors	40
4.1.1 Shape Features.....	40
4.1.2 Texture Features.....	41
4.1.3 Color Features	41
4.2 Classifiers.....	42
4.2.1 Support Vector Machines (SVM)	42
4.2.2. Artificial Neural Networks (ANN)	43
4.2.3 Deep Learning Methods	44
Chapter 5 Proposed System Evaluation and Results	46
5.1 Datasets Used.....	46
5.2 Proposed Algorithm/ Approach	48
5.2.1 Preprocessing of Digital Dermoscopic Images	49
5.2.2 Autonomous Segmentation of the Cancer Mole	49
5.2.3 Merged Segmentation Results.....	50

5.2.4 Similarity Measures.....	50
5.2.5 Feature Extraction	51
5.2.6 Feature Selection and Classification	51
5.2.7 Results	52
5.3 Software Used.....	52
5.4 Test Cases and Graphical User Interface (GUI)	53
5.5 Merged Approach for Binary Mask Computation	55
5.6 Results.....	60
5.6.1 Binary Mask Similarity Results from ground truth.....	60
5.6.2 Classification Results	61
5.7 Quantitative Comparison of Diagnostic Results with Published Systems.....	64
5.8 Advantages of Proposed Research work.....	66
5.9 Challenges of Proposed Research work.....	66
Chapter 6 Deep Learning Methodologies for Skin Cancer Classification.....	67
6.1 Datasets Used.....	67
6.2 Deep Learning Libraries Used	67
6.2.1 TensorFlow™.....	68
6.2.2 NVIDIA DIGITS.....	68
6.3 Deep Learning Models.....	68
6.3.1 Inception v3 Model	69
6.3.2 Alexnet Caffe Model.....	69
6.4 Hardware Requirement	70
6.5 TensorFlow Training and Classification Results	70
6.6 NVIDA DIGITS Training and Classification Results	75
6.7 Comparison Chart between DNN and ANN.....	81
6.8 Advantages of Deep Neural Networks (DNN)	82
Chapter 7 Conclusions	83
7.1 Merged Approach for Skin Lesion Segmentation	83
7.2 Parallel Classifier System	83
7.3 Deep Learning Methodologies for Skin Cancer Classification	84
7.4 Future Work	84
Bibliography	85

List of Abbreviations

S.No	Abbreviation	Explanation
1.	ALDS	Automatic Lesion Detection System
2.	DNN	Deep Neural Networks
3.	ANN	Artificial Neural Networks
4	SVM	Support Vector Machines
5	CNN	Convolution Neural Networks
6	CAD	Computer Aided Diagnosis
7	BCC	Basal Cell Carcinoma
8	SCC	Squamous Cell Carcinoma
9	FDA	Food and Drug administration
10	MRI	Magnetic Resonance Imaging
11	CT	Computed Tomography
12	ROI	Region of Interest
13	GLCM	Grey Level Co-occurrence Matrices
14	SSIM	Structural Similarity Index
15	CPU	Central Processing Unit
16	GPU	Graphical Processing Unit
17	GUI	Graphical User Interface
18	CUDA	Compute Unified Device Architecture

List of Tables

S.No	Table No	Details
1	Table 2.1	CAD System for Skin Cancer Detection and Classification
2.	Table 5.1	Dataset
3.	Table 5.2	Binary Mask Similarity Results
4.	Table 5.3	Classification Rules
5	Table 5.4	Classification Results using SVM
6	Table 5.5	Classification Results using Neural Classifiers
7	Table 5.6	Quantitative Comparison Table of Published System with Proposed System
8	Table 6.1	Classification Results using TensorFlow Library
9	Table 6.2	Classification Results using NVIDIA DIGITS Library

List of Figures

S.No	Figure No	Details
1.	Figure 2.1	Overall layers structure of human skin displaying all the three layers which are epidermis, dermis and hypodermis
2.	Figure 2.2	Nodular Basal Cell Carcinoma (BCC) sample cases
3.	Figure 2.3	Squamous Cell Carcinoma (SCC) sample cases
4	Figure 2.4	Melanoma mole sample case with irregular boundary and mix color variation
5	Figure 2.5	Chart representing the increasing number of skin cancer cases in previous and upcoming years
6	Figure 2.6	Dermoscopy instrument for the evaluation of pigment mole on any part of human skin.
7	Figure 2.7	a, and b shows the analog dermoscopes which are commercially available in the market.
8	Figure 2.8	Extensive classification between the normal and melanoma mole utilizing ABCDE clinical diagnosis method for skin tumor classification
9	Figure 3.1	Performance of DullRazor software on test case [33, 34], a) shows the darks hairs on lesion mole, b) shows the results with removed hairs using DullRazor software [14].
10	Figure 3.2	Sobel edge detector applied on test case image from DermQuest database [34] a) The original test case image, b) mole edges traced out using sobel edge detection method.
11	Figure 3.3	Overall algorithm of multistage canny edge detector with inputs $f(x, y)$ and outputs $g(x, y)$
12	Figure 3.4	Active contour model iterative process to lock onto nearby edges of the lesion area by minimizing the cost energy function
13	Figure 3.5	Active contour algorithm applied on test case image from DermQuest database [34] a) The original test case image, b) image converted to grayscale and lesion boundary segmented out using active contour method

14	Figure 3.6	Watershed segmentation valley is associated with a catchments basin, and each point in the landscape belongs to exactly one unique basin
15	Figure 3.7	Watershed algorithm applied on test case image from Dermis database [33] a) The original test case image, b) image converted to grayscale and lesion boundary and mole segmented out using watershed segmentation
16	Figure 4.1	Neural network interconnected layers (input, hidden and output) architecture
17	Figure 4.2	Three-layer deep neural network interconnected layers (input, hidden and output) architecture
18	Figure 5.1	Proposed algorithm of the overall automatic lesion detection system (ALDS) for skin cancer classification
19	Figure 5.2	Test cases for the proposed research work for which binary mask will be segmented and classification results will be generated
20	Figure 5.3	Images under changed lightning conditions a) good lightning condition b) & c) inappropriate lighting condition
21	Figure 5.4	GUI for the proposed research work, a) active contour GUI, b) main evaluation GUI
22	Figure 5.5	Overall watershed algorithm process applied to test case (b) of Figure 5.2
23	Figure 5.6	Overall active contour iterative process a) process applied to test case (f) of Fig 5.3, b) the image is converted to gray scale image, c) the process iterates for 250 times, d) the process iterates for 500 times, e) the process iterates for 1000 times, f) after 1000 iterations final active contour binary mask is generated
24	Figure 5.7	Overall merged process using individual watershed and active contour binary mask applied to test case (b) of Fig 5.2
25	Figure 5.8	Test images along with their original mask, active contour mask, watershed mask and merged mask (Dataset [32-34])
26	Figure 5.9	Six different cases of different categories with masks loaded on actual test images.
27	Figure 5.10	Artificial neural classifier, a) overall neural network with 10 hidden neurons, b) confusion matrix with 80% accuracy rate, c) ROC curve

28	Figure 6.1	Detailed Inception model layer architecture which includes convolution layer, avgpool layers, maxpool layers, concat layers, dropout layers, fully connected and softmax layers
29	Figure 6.2	Detailed Alexnet model layer architecture which includes input layer, convolution layer, pool layers, fully connected (FC) layers and softmax layers
30	Figure 6.3	Folder containing two main classes of skin cancer training images categorized as melanoma and non-melanoma
31	Figure 6.4	Google Inception v3 network creating bottleneck values against each image in training folder divided in to two main classes melanoma and non-melanoma in text format
32	Figure 6.5	The retraining process of Google Inception v3 network with final train accuracy of 100 % and test accuracy of 83.4 %.
33	Figure 6.6	The detailed (a) accuracy and (b) cross entropy graph of TensorFlow library for 4000 iterations.
34	Figure 6.7	The test case folder containing test cases images in RGB format from both melanoma and non-melanoma classes
35	Figure 6.8	The skin cancer training dataset for training the state of the art Caffe Alexnet model.
36	Figure 6.9	The Malignancy-Measure model using Caffe Alexnet model for classification between melanoma and non-melanoma cases
37	Figure 6.10	The training process of Malignancy-Measure model using Caffe Alexnet model with final train accuracy of 81% and training loss of 2%
38	Figure 6.11:	Detailed results (a), (b), (c), (d), (e) and (f) for test case 3 with statistical parameters.

Chapter 1

Introduction

Cancer now a days is one of the greatest growing group of disease throughout the world. Among which skin cancer is most common of them. It happens due to the abnormal growth of cells with chances to spread over the other parts of body. According to stats and figures annual rate of skin cancer are increasing each year [55]. The modern medical science and treatment procedures proves that if the skin cancer is detected in its initial phase then it is treatable by using appropriate medical measures which includes laser surgery or removing that part of skin which ultimately saves patient live. Technology advanced platforms help in detecting any type of skin cancer in its initial phase. These platforms are based on advanced computer vision, deep machine learning and pattern recognition techniques. The overall thesis is based on detailed study and utilizing state of the art algorithms and approaches for skin cancer detection and classification using digital dermoscopy images from three different datasets [15, 32, 33, 34]. The proposed research work presents a novel method for Automatic lesion detection system (ALDS) for precise and accurate skin cancer classification.

1.1 Problem Statement

As discussed in previous section that annual rate of skin cancer is increasing every year and if it is detected and treated using appropriate medical measures in its early phase then we can save patients life. Skin cancer has two main stages which includes malignancy and melanoma among which melanoma is fatal and comes with the highest risk. In most of cases malignant mole is clearly visible on patient's skin which are subsequently identified by the patients themselves.

Technology advanced platforms help in detecting malignant moles on any part of skin by taking the advantage of computer aided diagnosis systems. Computer aided diagnosis system is not only used for skin cancer detection but for many other diseases [16] among which most of the diseases are of severe category. Computer aided diagnosis system are based on advanced computer vision, deep machine learning and pattern recognition algorithms for disease detection and classification.

Dermoscopic diagnosis refers to non-invasive skin imaging method, which has become a core tool in diagnosis of melanoma and other pigmented skin lesions. It includes optical recognition of region of interest (ROI) thus making it more clear and visible for the dermatologists to analyze the case under consideration. However, dermoscopy using conventional method may lower down the diagnostic accuracy which can lead towards the more chances of errors. These errors are generally caused by the complexity of lesion structures and subjectivity of visual interpretations [7].

To minimize the chances of error and achieve a professional diagnostic approach an automated analysis of dermoscopy image includes following steps. Preprocessing of digital image which includes removing clutter such as hair from that part of the skin where pigmented mole is present, applying the sharpening filter to make that area more clear and visible. The next essential step is automated segmentation of region of interest where the malignant mole is present by using state of the art based computer vision methods. The last step includes the feature extraction and classification process to extract the results for the case under consideration.

The problem addressed in this thesis is how to analyze the provided digital dermoscopic image for the correct segmentation of pigmented network on any part of body. In the next step the segmented mole will be further classified by utilizing state of the art classification system for precise and accurate extraction of the outcomes for the coveted case. The datasets used for the proposed research work are collected from PH2 database [15, 32], Dermis database [33] and DermQuest database [34].

1.2 Thesis Structure

The rest of the thesis is arranged as follows

Chapter 2 includes literature review about human skin and skin cancer from medical point of view. The last part of this chapter is about available commercial computers diagnosis systems which are being widely used. Chapter 3 and Chapter 4 presents the methods and approaches used for skin cancer mole segmentation and classification from research areas of computer vision, pattern recognition and machine learning. My contribution and work for automatic lesion detection system (ALDS) for skin cancer classification using support vector machines and neural classifier is reflected in chapter 5. This chapter presents a novel hybrid approach for pigmented mole segmentation and parallel classification system for extracting results in the form of likelihood of malignancy. The last part of this chapter includes the advantages and challenges of proposed work. Chapter 6 introduces advanced deep learning frameworks based on deep neural networks (DNN) for accurate and robust classification between non-melanoma and cancerous moles (melanoma). Chapter 7 concludes the thesis and sum up my contribution toward the field of computer aided diagnosis systems.

Chapter 2

Background

This chapter presents a detailed literature review on different aspects of human skin and skin cancer. The first part of the chapter describes human skin from medical point of view which further goes towards layers of human skin. The second part focuses on biology of skin cancer disease, its types and stages, treatable and non-treatable phases skin cancer. The next part of this chapter introduces dermoscopy and different clinical diagnosis methods or approaches which are used to detect and classify the cancerous mole on human skin. The last and final part of the chapter gives us the description of commercial computer aided diagnosis systems which are being used in medical fields.

2.1 Human Skin Biology

The human skin is the largest organs of the overall human body. It covers all others organs of body. It guards the entire body from microbes, bacterium, ultraviolet radiations helps regulate body temperature, and permits the sensations of touch, heat, and cold [51]. Human skin is a progressive organ and it undergoes gradual changes at different stages of human life. The thickness of human skin varies from eyelids which is 0.5mm to palm of the hands and soles of feet which is 4mm [5]. Male skin is thicker as compared to female skin throughout the entire body. Human skin is divided into three main layers which are epidermis, dermis and deeper subcutaneous issue [41].

2.1.1 Human Skin Layers

There are three main layers of human skin which are as follows

- Epidermis
- Dermis
- Hypodermis / Deeper Subcutaneous issue

Epidermis: The outermost and also the top layer of human skin is known as epidermis. This layer is made up of flat, scale like cells also known as squamous cells. Basal cells are next level cells which are under the squamous cells.

Dermis: It is the layer between epidermis and Deeper Subcutaneous issue. It consists of dense irregular connective tissue, the dermis layer contains three major type .of cells which are fibroblasts, macrophages, and adipocytes. This layer also contains special cells which are used to repair the damaged skin.

Hypodermis: This is the layer between the outer skin and the inner muscle tissue. It consists of fat cells and does have blood vessels and nerves passing through it. It helps insulate the body from cold and provides cushion for the deep tissues from blunt trauma. It can also serve as a reserve fuel source for the body [40].

The [Figure 2.1](#) shows a descriptive image of all the layers of skin

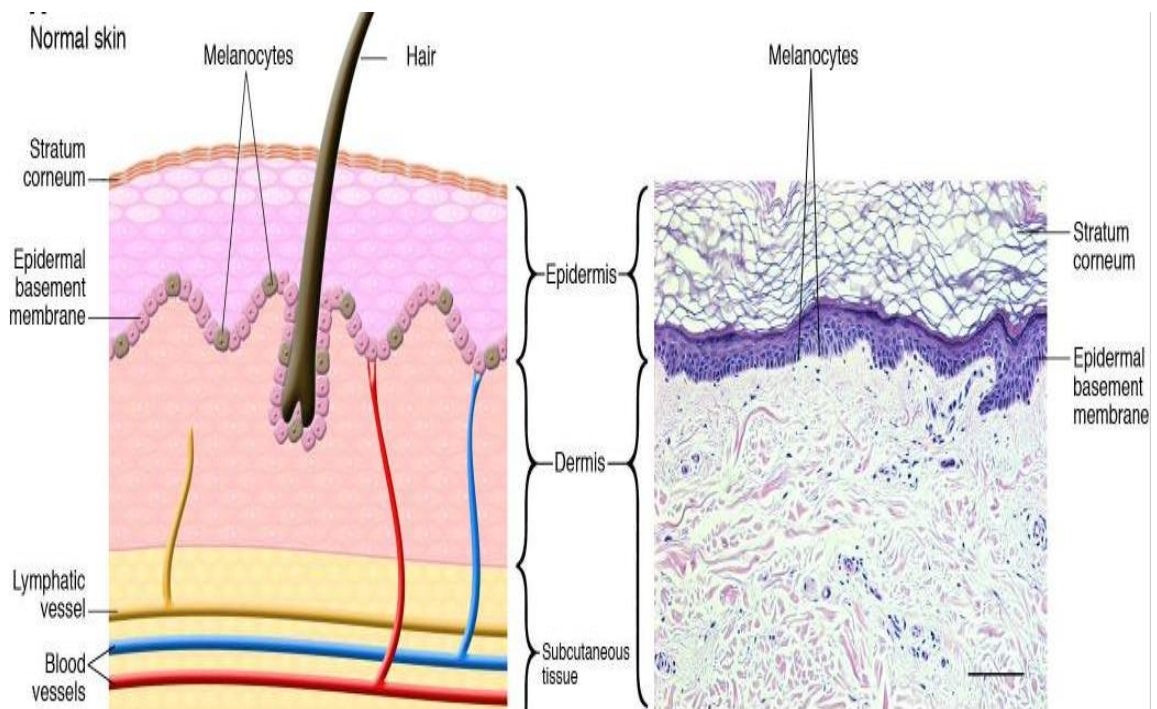


Figure 2.1: Overall layers structure of human skin displaying all the three layers which are epidermis, dermis and subcutaneous tissue [12]

2.1.2 Types of skin moles

A mole or nevus on human skin can be described as a dark, erected spot comprised of skin cells which are grown in a group rather than individually. These cells are generally known as melanocytes which are responsible for producing melanin, the pigment color in our skin.

Moles on human skin can be from birth also known as birth mark or it can progress by time beings. The major and prior reason behind mole development on human skin is predominantly because of direct sun exposure and any kind of extreme injury. Fair skin population have greater ratio of skin moles due to the lower quantity of melanin (natural pigments) in their skins [69]. There are many different types of moles on human skin which are as follows

- Common mole
- Atypical mole
- Congitel mole
- Acquired mole
- Junctional melanocytic nevi
- Compound nevi

2.2 Skin Cancer

Cancer mole on skin is a most frequently befalling malignancy in fair skinned population. There are three basic types of skin cancer, which includes Basal Cell Carcinoma (BCC), Squamous Cell Carcinoma (SCC), and Melanoma. Malignancy is a description of the “stage” of cancer. All of these cancers are fatal however Melanoma comes with the highest risk and found very frequently in the fair skinned people aging less than 50 years for men and more than 50 years for women [57]. Skin cancer starts producing in the form of cells which finally progresses in tissue structures. The most important thing from a doctor’s point of view is to distinguish and flawlessly identify lesion area. Failure to correctly identify and subsequent delayed treatment of a lesion may lead to advanced stages of cancer. Therefore, early detection is of major importance for the dermatologists. In the process of skin cancer screening, clinicians usually detect the suspected lesion region by visual checkup and manual measures known as biopsy test. The term biopsy refers to procedure in which dermatologists takes the sample of infected tissues to examine them more closely, after which they come up with results for the case under consideration. However visual checkup is highly dependent on observer skills and is likely to have human error. In European and American countries, it is highly emphasized to the clinicians to have careful attention and precision in distinguishing and analyzing the skin cancers [3]. Hence by the evolution of improved algorithms and techniques, clinicians may seek “second opinion” from the Automatic Lesion Detection System (ALDS) based on computer aided diagnosis software to refine their diagnostic performance.

2.2.1 Types of skin cancer

There are three types of skin cancers which are as follows

- Basal Cell Carcinoma (BCC)
- Squamous Cell Carcinoma (SCC)
- Melanoma

Basal Cell Carcinoma (BCC): It is the most common type of skin cancer and it grows in the skin cells which are known as basal keratinocytes which are found in the deepest layer of epidermis. It is also known as rodent ulcer and basalioma. Patients with BCC often develop multiple primary tumors over time. The important characteristic of BCC includes the following. Firstly, it is a gradually growing nodule and it is commonly pink in color, secondly it has different size variation which can be from few millimeters to centimeters in diameter and in most cases, it results in bleeding or ulceration [24]. [Figure 2.2](#) represents the nodular BCC cases

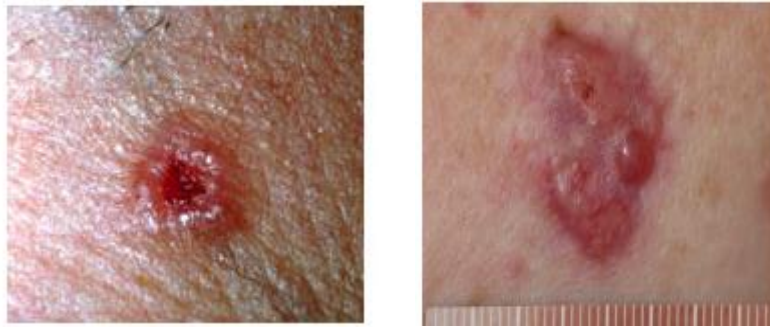


Figure 2.2: Nodular Basal Cell Carcinoma (BCC) sample cases [24]

Squamous Cell Carcinoma (SCC): The next most common type of skin cancer is squamous cell carcinoma. It is also due to the abnormal growth of cells which leads towards formation of infected tissues. It mostly grows on skin upper layer epidermis. SCC can grow on any part of skin. But it mostly infects the skin regions which are directly exposed to sun rays, therefore doctors and dermatologist often advice their patients to cover those parts of body which can become be affected by ultra violet radiations. The advanced stages of invasive SCC has metastatic potential and can be fatal. The important characteristic of SCC is it exposes the telltale signs of sun damage, including wrinkles, loss of elasticity, pigment changes, freckles, and broken blood vessels [62]. [Figure 2.3](#) represents SCC case

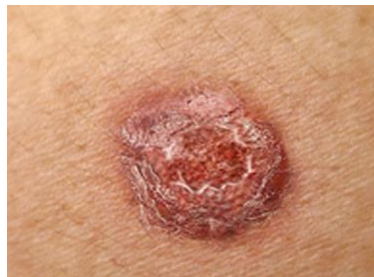


Figure 2.3: Squamous Cell Carcinoma (SCC) sample cases [61]

Melanoma: It is third and most serious type of skin cancer. Although basal cell carcinoma, squamous cell carcinoma and melanoma all of these types of cancer are fatal however melanoma comes with the highest risk. The main cause of melanoma is direct exposure to dangerous ultraviolet radiation from sun on any part of body. Melanoma can grow on any part of body however this type of cancer can also form in eyes. The risk factor of melanoma is more in people aging less than 40 especially in women [46]. The important characteristic of melanoma includes color variations and irregular borders. If melanoma is diagnosed in its early stages it can be treated by using appropriate medical measures. Melanoma moles have different color variation which includes particularly black and brown color shades [Figure 2.4](#) represents a melanoma case



Figure 2.4: Melanoma mole sample case with irregular boundary and mix color variation [33-34]

2.2.2 Skin Cancer Facts and Statistics

Skin cancer is most dangerous and fatal type of disease and the chances of melanoma skin cancer increases with the growing age. Some important skin cancer facts and statistics are discussed as follows. Every hour one person dies due to melanoma. During the recent few years, the frequency of melanoma treatment cases has increased extensively, lasting at the top in all the cancers with respect to its management [47, 56]. About 76,380 new cases of melanoma (46,870 for males and 29,510 for females) and about 10,130 cases of new melanoma related life expires are expected during the year 2016 in the United States [54]. Skin cancer is one of three cancer with increasing rate especially in men along with liver cancer and esophageal cancer. More than one million squamous cell carcinoma cases are diagnosed each year in US. According to World Health Organization (WHO) every year about 232,000 cases of melanoma are detected each year through worldwide [54]. Non- melanoma skin cancers, such as Squamous Cell Carcinoma (SCC) or Basal Cell Carcinoma (BCC), contribute to the substantial indispositions among fair

skinned Asians. The Figure 2.5 chart shows the increasing number of cancer cases in previous and upcoming years.

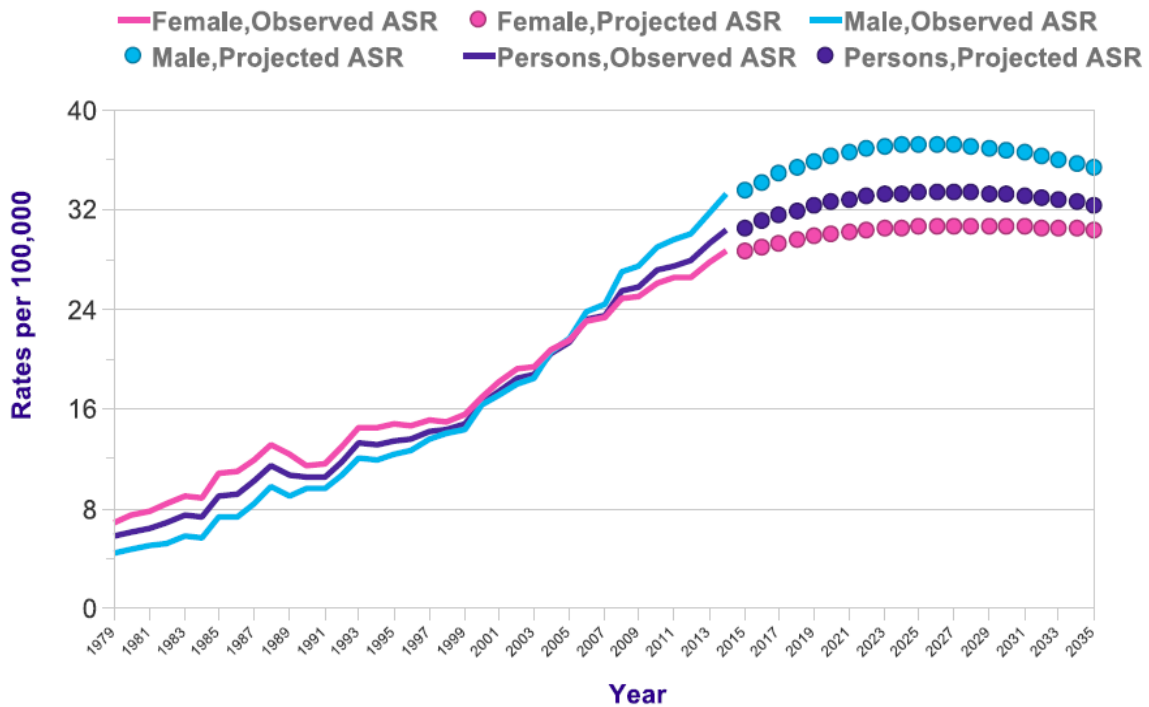


Figure 2.5: Chart representing the increasing number of skin cancer cases in previous and upcoming years (Statistics reprinted with citing permission [27]).

2.2.3 Skin Cancer Treatments

As it is discussed in chapter 1 introduction section that if the skin cancer is diagnosed and treated in its initial phase using appropriate and possible medical measures it can be cured. Since Basal Cell Carcinoma and Squamous Cell Carcinoma are non-melanoma skin cancer medical science proposed certain methods which are used for treatments of these types of skin cancers. During the surgical procedures, local anesthetic is used by the specialists. The methods used for skin cancer treatments are as follows [58]

- Micrographic Surgery
- Excisional Surgery
- Electro Surgery
- Cryosurgery
- Radiation
- Photodynamic Therapy
- Laser Surgery
- Topical Medications

Although the treatment of Squamous Cell Carcinoma (SCC) and Basal Cell Carcinoma (BCC) are treatable but it purely depends on malignant mole size. The greater the size of mole the more extensive treatment is required. Laser Surgery and Radiation therapy are one of the most common and widely used method for skin cancer treatments

2.2.4 Prevention from Skin Cancer

Prevention is the key element to get protected and cured form any severe disease. The same rule follows in the case of skin cancer and it is the major action to minimize the chances of progress of malignant mole on any part of body. Eventually it lower the death ratio due to skin cancer. Doctors and dermatologist usually prefer their patients to prevent themselves by using different methods especially in fair skinned populations. These methods are as follows [52]

- Try to remain in shady areas especially during the peak hours of day from 10 am to 4 pm.
- Try to cover up the entire body with clothes as skin cancer can grow on any part of skin.
- It is highly preferred to keep newborn babies out of ultraviolet sun radiations.
- Visual checkup s and skin examination test is compulsory from head to toe every month.
- Moreover if there is any type of mole other than cancer mole such patients must visit their doctors for precautions checkups.
- One must use sunscreen to cover their face for prevention from ultraviolet rays.
- Smoking is one of the cause of skin cancer therefore one should avoid smoking.
- Healthy diet is compulsory for skin cancer prevention
- Exercise on regular bases plays a key role from prevention not only from skin but almost all of the diseases.

2.3 Dermoscopy

Dermoscopy refers to non-invasive skin imaging method, which has become a core tool in diagnosis of malignant melanoma cases and other pigmented skin lesions. It is the diagnostic approach based on the evolution of color variations and observations of microstructures of the epidermis and papillary dermis which is not visible to naked eyes. In dermoscopy the lesion mole (region of interest) is greased with alcohol or oil in order to reduce the skin reflectivity and increase the transparency of lesion mole. After applying the liquid material, the lesion mole is examined under the specialized optical system. The dermoscopic tests helps the doctors and dermatologists to effectively differentiate between melanoma and other pigmented lesion mole [38]. Specialized optical systems which are

used for performing dermoscopy test includes led light system with polarization also known as polarized light test.

.Dermoscopic elements are widely used throughout the world for better diagnosis and early detection of skin cancer. [Figure 2.6](#) shows the dermoscopic instrument for mole diagnosis



Figure 2.6: Dermoscopy instrument for the evaluation of pigment mole on any part of human skin (Figure reprinted with citing permissions [72])

2.3.1 Digital Dermoscopy

Dermoscopic test can be divided in two major types which includes analog dermoscopy and digital dermscopy. Digital demoscopic test is easier to perform as compared to analog dermoscopic test. The outcomes got from computerized dermoscopic test are more accurate as they uses particular and specialized camera image capturing feature. For digital dermoscopic tests high quality mole analyzers and digitized photography instruments are used with especial type of digital zoom lens. Analog dermoscopic instruments can be attached to digital camera in order to provide the advantage of digital dermoscopy. Heine Delta 20®, DermLite III DL3®, Dermogenius® and DermLite II Pro® are analog dermoscopes commercially available in the market, which are accordingly shown in [Figure 2.7](#). Digital dermoscopes includes DinoLite and Handyscope which are commercially available in the market.



(a) DermLite III DL3®



(b) Dermogenius®

Figure 2.7: Analog dermoscopes (a) and (b) which are commercially available in the market (Figure reprinted with citing permissions [72])

2.4 Clinical Diagnosis Techniques

This part of chapter will discuss different clinical diagnostic techniques which are most commonly used for classifying between cancerous malignant mole with benign mole or normal mole. These techniques include Menzies method, CASH algorithm, Seven point checklist method and ABCD method for skin cancer detection

2.4.1 CASH Rule

The word CASH is combination of four important features where C stands for Color, A for Architecture, S for symmetry and H for homogeneity vs heterogeneity [29]. In order to correctly classify the case under consideration whether it's a malignant mole or benign mole dermatologist look for these four features. If the color of the mole varies between different color shades like brown, black, red, white, blue then it is the possible symbol of cancerous mole. Second important feature is the architecture of lesion area which can be described as its order vs disorder. If the mole progresses in disorder type then it is the symbol of cancerous mole. The third feature according to this rule includes the symmetry of the lesion mole. If the structure of mole is not symmetric either in one or both axes then it is the possible symbol of cancerous mole. The last feature includes the homogeneity vs heterogeneity structure of the lesion mole. If the mole structure consist of streaks, blotches, regression, globules, blue white veil then the mole can be cancerous mole [29].

2.4.2 Seven Point Checklist Method

The second most important technique which has gained greater interest among dermatologists is the seven-point checklist method for skin cancer classification. This method also extracts seven features which is further used to classify the case under consideration as malignant or benign mole. These seven features are divided into three major signs and four minor signs for precise and accurate classification of cancerous mole. The three majors signs includes change in size, change in shape and change in color, The four minor signs include inflammation, bleeding, sensory change and diameter of mole [31].

2.4.3 Menzies Method

Menzies method is type of pattern analysis technique which is used for skin cancer classification. Menzies method extract the classification results by providing two negative feature and nine positive feature. The case under consideration falls in the category of normal or benign mole if two negative feature are present which includes symmetry of the mole and presence of single color. Whereas it falls in the category of malignant melanoma if one or more positive feature are presents which includes multiple brown dots, blue white

veil, radial streaming, globules, presence of multiple colors, uneven borders, pseudopods, multiple gray dots and scar like depigmentation [30].

2.4.4 ABCD Method

The ABCD method for skin cancer classification is one of the most widely used method and it is understood as backbone of all methods. The ABCD method is combination of four core features for classifying between melanoma and normal mole. These four feature are abbreviated as ABCD where A stands for asymmetry, B for border evolving, C for color variation and D for diameter of the mole. If the mole is not symmetrical means its asymmetrical then it is the possible symbol of cancerous mole. Secondly if the border structure of pigmented area is not even then it is the symbol of cancerous mole. The third feature includes the color formation of lesion area. If the color of the mole varies means it is the combination of one or more colors then it is the possible symbol of cancerous mole. The last but not least is the diameter of the mole. If the diameter of the mole is greater than 6mm then it is the possible symbol of cancerous mole [28]. ABCDE is advanced form of ABCD method where one more E feature is added. It stands for evolving of the mole. This feature computes the continues change in size, shape and color of the mole with respect to time. The Proposed research work will focus on ABCD method for skin cancer classification which will be later discussed in chapter 5. The [Figure 2.8](#) represents the comprehensive classification between normal and melanoma case using ABCDE method.

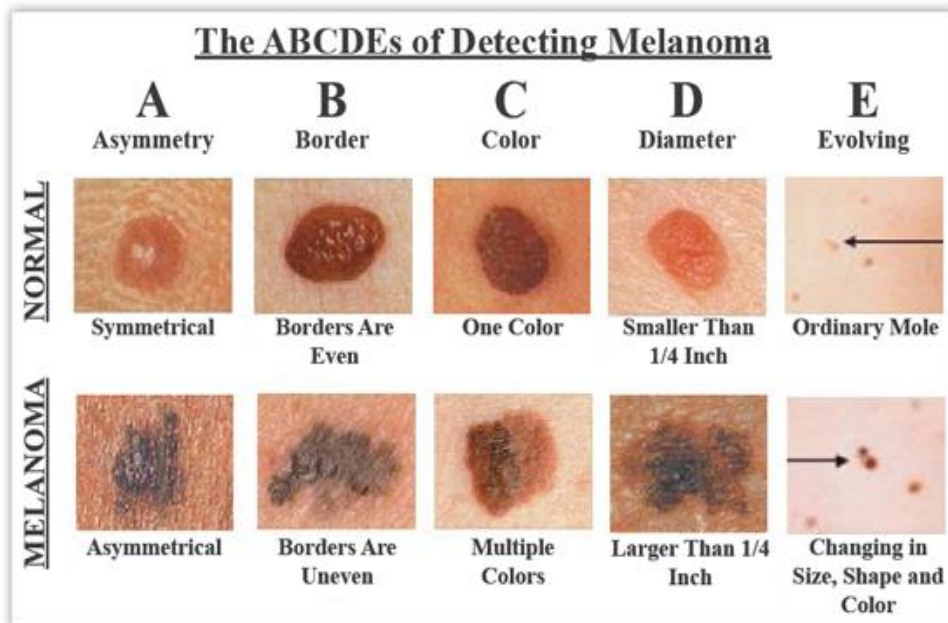


Figure2.8: Extensive classification between the normal and melanoma mole utilizing ABCDE clinical diagnosis method for skin tumor classification [39]

2.5 Computer Aided diagnosis (CAD) Systems

In the 1980s, different approaches of computer systems were emerged for the development phase of computer aided detection and diagnosis system which could be utilized by radiologists, for disease diagnosis. This concept is currently known as computer-aided diagnosis system, which has been widely and quickly spread throughout the world and different. But according to some computer scientists such type of system would not work due to not sufficient and advanced technological platforms. Moreover reason for this strong criticism at that time might have been related to an unsuccessful attempt in previous research, efforts toward the development of automated computer diagnosis. This seems to indicate that a failure of a specific research project can lead to a strong “incorrect” bias toward another area of research that may look similar to the failed previous research. However as the time passed more advanced and robust computer aided diagnosis system came in the development phase to achieve more robust accuracy levels [7].

It inherits the concepts of pattern recognition, computer vision and image analysis capabilities. CAD systems are basically used to mark regions of an image that might reveal specific abnormalities and alert the clinician to these regions during image interpretation. Computer-aided diagnosis (CADx) systems aids the professionals about specific diseases, disease type, severity, stage and progression.

Quantile image analysis (QIA), has been recently developed. Using technologically advancement tools, it extracts quantitative imaging biomarkers from medical images. A quantitative imaging biomarker is an objectively measured characteristic derived from an in vivo image as an indicator of normal biological processes, pathogenic processes or a response to a therapeutic intervention. Quantitative imaging includes the development, standardization and optimization of anatomical, functional and molecular imaging acquisition protocols, data analyses, display methods and reporting structures.

Computer aided design and QIA both share numerous basic parts and both use a richness in medical imaging that still can't seem to be completely tapped. There is a characteristic cooperative energy between the two and we expect that systems created in one field are probably going to be pertinent in the other. Additionally, both strategies can profit by institutionalized evaluation and subsequent advancement in medical imaging technology.

Extensive scale and precise innovative work of different CAD system plans were started in the mid-1980s at the Kurt Rossmann Laboratories for radiographic images research at Chicago University [7]. From that time, the ongoing research is being carried on to develop more efficient CAD systems. The greater impact of advance medical imaging has taken the CAD system to next phase of high level accuracy and robust performance. As the modern technology is advancing by leaps and bounds the trend of computer aided diagnosis system is becoming more common in medical industry. Doctors and specialists highly prefer such type of systems as it reduces the chances of error and can be used as second opinion. Computer aided diagnosis systems follows the Moore's Law according to which computation power doubles each year. Faster and reliable computational hardware systems

allows immense computing power and secure database systems. Software system improvement plays a vital role in development of CAD systems. CAD systems are widely used for diagnosis of different diseases which includes lungs cancer, different eye diseases, chest diseases and many more among which are described below

2.5.1 Lung Nodule Detection and Chest Radiography

For chest radiography, many different computer aided diagnosis system have been developed and some of them are commercially available in the market. In chest radiography the cad system works by detecting and diagnosing the lung nodule, detection of pneumothorax, cardiomegaly, and interval changes. Lateral view is generally used as the supporting method to increase the performance of CAD system for the detection of lung nodule.

Recently, Shiraishi et al has designed a system which can be used to detect the lung nodules in lateral views of chest radiography. In PA (posterioranterior) views the overall sensitivity in lung nodule detection is 70.5% and when lateral views were used the sensitivity decreases to 60.7% with 1.7 false positives per image [7].

2.5.2 Intracranial Aneurysms Detection in MRA

Medical imaging regarding the computed tomography angiography (CTA) and magnetic resonance angiography (MRA) has achieved more interest in past few years. It is still considered a complex tasks for doctors and professionals to find small aneurysms and sometimes the detection of medium size aneurysm also become the complex task. By using CAD system such type of difficulties can be overcome by aiding the radiologist in the detection of intracranial aneurysms. [7]

2.5.3 Interval Changes Detection in Whole Body Scans

Bone scintigraphy is the most successive examination among different nuclear-medicine prescription strategies. It is a settled imaging methodology for the conclusion of rigid metastases and for observing of the bone tumor reaction to chemotherapy and radiation treatment. In spite of the fact that the affectability of bone output examinations for recognition of bone variations from the norm conditions has been thought to be high and considered as most time-consuming tasks. To cater such type of challenges Shiraishi et al. built up a CAD system for the recognition of interim changes in progressive entire body bone sweeps by utilization of a fleeting subtraction picture which was acquired with a nonlinear image-warping procedure. It consists of steps which includes image normalization, image matching of all the paired images and feature extraction. [7]

2.6 Computer Aided diagnosis (CAD) Systems for Skin Cancer Detection and Classification

Several computer aided diagnostic systems have been developed for early skin cancer detection based on the modern image processing and computer vision algorithms such as ABCD rule of dermoscopy, Menzies Method, 7-Point Checklist and the CASH algorithm [26]. Such systems work by collecting important features of lesion and produces the results on the basis of these feature values. Some of the commercial computer aided diagnosis system for skin cancer detections systems includes solar scan, molamax, melafind. and siascope. The details of these systems is discussed in the below sections.

2.6.1 SolarScan

SolarScan® monitoring system is a type of advance skin imaging systems used by dermatologists and specialists to precisely analyze different skin diseases along with skin cancer. The system was built by the merged corporation of Polartechnics Limited, Sydney melanoma unit and Commonwealth Scientific and Industrial Research Organization (CSIRO) [59]. SolarScan system is advanced enough to analyze and detect even very minute changes in a mole. The system works by taking the advantage advances photography of the lesion area with a built in surface microscope. The images are then refined by image analysis software by removing clutters like hairs and oil bubbles. In the next step the system computer different mole features which includes size, shape and color which are then compared against the features of melanoma non-melanoma cases stored in the system database. The system finally stores the results of case under consideration which can be rechecked if required in future. The systems achieves overall sensitivity of 91% and specificity of 68% for melanoma cases [18].

2.6.2 MoleMax

MoleMax II scanner system was developed by the University of Vienna. It is counted as state of the art system for skin cancer diagnosis in early phase. The system has built in ability for very high magnification along with special light frequency that allows the doctors and dermatologists to carefully examine the lesion area skin structure. The MoleMAX system lists in world leading medical technologies. MoleMax II is the first integrated system for digital epiluminescence microscopy and macro imaging in the world. The system is highly preferred among the research community and dermatologists for its precise and accurate classification abilities. The system comes with state of art image analysis functions which includes comparison of the case under consideration with reference images stored in system database. The system works on ABCD and new seven point check list method for early skin cancer classification [48].

2.6.3.MelaFind

MelaFind system was developed by medical company known as Mela Sciences. Like other commercial computer aided diagnosis system MelaFind is also used for early skin cancer detection and it provides addition information about atypical skin lesions during melanoma examinations. The system uses special light which has infrared wavelength for precise and accurate examination of lesion area of skin up to 2.5mm beneath the skin. This system has received bronz Edison award for its innovation and it is listed in top ten medical system in the year 2013. The system achieves high sensitivity rate of 98.3% and specificity between 70-85 % [18] for its precise and accurate classification for the cases under consideration. Food and Drug administration (FDA) authorizes Melafind System for product marketing in November 2011 [45]. The system uses predefined state of the art image analysis algorithm to correctly classify the case under consideration by providing negative and positive results.

2.6.4 SIAscope

It is type of noninvasive skin imaging handheld device most commonly used by dermatologists. The device helps to carry out the rapid screening test of the lesion skin area as well 2mm beneath the skin without the need of painful biopsy test. Along with handheld device the system comprises of powerful image analysis software that scans and visualizes hemoglobin, melanin, dermal melanin and collagen up to 2 mm under the skin and provides the classification results [48].

2.7 Comparison of Computer Aided diagnosis (CAD) Systems for Skin Cancer Detection and Classification

The below table represents different published CAD systems for skin cancer detection and classification and state of the art algorithms which are being applied for respective area of interest

TABLE 2.1: CAD System for Skin Cancer Detection and Classification

S.no	Paper Title	Medical Imaging Category	Arear Of Interest	Algorithm's Applied	Accuracy
1.	A Combined Segmentation	Dermoscopic images	Lesion Detection	Median filtering and	-

	Approach for Melanoma Skin Cancer Diagnosis [19]			active contour methods	
2.	Nuclear Segmentation For Skin Cancer Diagnosis From Histopathological Images [17]	Histopathological Images	Segmentation and Classification	C- means algorithm and neural classifiers	
3.	SVM based Texture Classification and Application to Early Melanoma Detection [22]	Dermoscopic images	Classification	Support Vector Machines (SVM)	70 %
4	Computer aided Diagnosis of Melanoma Using Border and Wavelet-based Texture Analysis [11]	Dermoscopic images	Classification	Support Vector Machines and Logistics model tree	91 %
5	Set Of Descriptors For Skin Cancer Diagnosis Using Non-Dermoscopic Color Images [13]	Non-Dermoscopic Images	Classification	Artificial Neural Networks (ANN)	76 %

2.8 Proposed Computer Aided diagnosis (CAD) Systems for Skin Cancer Detection and Classification

The proposed research work focuses on development of CAD system for skin cancer detection and classification tasks using conventional dermoscopic images. The systems

utilizes novel merged segmentation approach for lesion detection and state of the art classifier system for accurate classification of test under consideration which is later discussed in chapter 5 and chapter 6. The proposed systems have been practiced using the research findings of Chang et al [3]. Chang et al [3] system is based on manual pen based segmentation approach which has chances of error whereas the proposed work utilizes automated merged approached of watershed and active contour algorithms for accurate and precise segmentation of lesion area. Secondly for the classification of the segmented mole we have utilized Support Vector Machines (SVM) and Artificial Neural Networks (ANN) in complementary role. Deep learning methodologies is incepted for the proposed research work to increase the accuracy level as compared to conventional neural classifiers. In this way total five algorithms has been applied where two are used for mole segmentation and four are used for mole classification purpose respectively.

2.9 CAD System Future Potentials

Throughout the years, experts have been working on two unique sorts of CAD systems, one for detection and second for classifying in view of grouping amongst threatening and considerate sores, and furthermore between various ailments, for example, extraordinary interstitial lung illnesses, skin cancer classification In spite of the fact that CAD plans for identification of sores, for example, bosom sores on mammograms have been effectively actualized in clinical circumstances, no genuine endeavors have been made to apply CAD plans for differential diagnosis to practical clinical situations [7]. It is likely in future that CAD plans will be incorporated together with other specialized software's for medial image processing in the workstations related with some particular imaging modalities, for example, advanced mammography, CT, and MRI and dermoscopic images.

Chapter 3

Skin Lesion Segmentation Using Various Techniques

This Chapter will focus on advance computer vision techniques for automated segmentation of malignant skin lesion (Region of interest) used in medical technology to aid specialists and demonologist to increase their diagnostic abilities. The chapter will discuss different state of art algorithms for precise and accurate segmentation of dermoscopic images which include manual and automatic approaches. Manual method includes pen based segmentation method. On the other side automated approaches includes edge detection methods, region based segmentation techniques, clustering methods, connectivity preserving (active contours) techniques and watershed transformation method.

3.1 Automatic Lesion Detection / Segmentation Methods

This part of chapter will explain different state of the art algorithms widely used in medical imaging for the automatic segmentation of region of interest in dermoscopic images. The process continues after the pre-preprocessing of digital dermoscopic images. It includes removing clutters like hairs and extraneous skin for the accurate and precise segmentation of pigmented area. The last part of chapter will focus on the use of merged approaches to enhance the segmentation capabilities of image analysis software for the cases under consideration.

3.1.1 Preprocessing of digital dermoscopic images

Preprocessing of digital dermoscopic images is essential step for producing refined dermoscopic image that will be utilized by different automatic segmentation algorithms. Preprocessed dermoscopic images will ultimately help the automatic segmentation techniques to produce robust and rigid results. The first preprocessing step includes the removing of clutter which occurs in the form of dark hairs on the top of pigmented skin regions. It can causes confusion which can results in unsatisfactory segmentation conclusions. DullRazor [14] software is widely used for non-commercial purpose for

removing hairs from dermoscopic images. The software algorithm has been implemented in C language on a Sun OS 4.x workstations [14]. Figure 3.1 illustrates the effectiveness of DullRazor software by implementing the software on the lesion area covered with dark hairs



Figure 3.1: Performance of DullRazor software on test case [33, 34], a) shows the darks hairs on lesion mole, b) shows the results with removed hairs using DullRazor software [14].

3.1.2 Edge Detection Methods

In this method of image segmentation, we particularly focus on object boundaries contained within the image edges. Edges can be defined as discontinuity of intensities in the image. It is most common technique used for image segmentation There are four main types of edge detection methods which includes sobel row-edge detector, prewitt edge detector, laplacian of guassian also known as Marr-Hildreth method and last but not least is canny edge detector. Edge detection technique is widely used in many applications like object segmentation which includes face detection, used to locate object in satellite images like road, forest, different land areas, medical imaging which includes cancer mole segmentation, locate tumor and other pathologies, surgery planning. Moreover, it is also used in recognizing different object like face recognition and finger point recognition.

3.1.2.1 Prewitt and Sobel Edge Detector

These both edge recognition techniques work by processing the derivatives in x and y directions. In the following stride, it computes the gradient magnitude and lastly it finds the threshold estimation of gradient magnitude. Their fore these two methods are also known as gradient operators. Sobel edge detector first performs average smoothing in x and y direction to the input image which results in blurred image. Then it applies derivative filtering in x and y direction to detect the edges in the desired image. The only difference between sobel and prewitt edge operators is of derivative filtering. Sobel edge

detection method has quick performance but on the other hand it fails to detect weak edges. It has robust performance in the absence of noise. From medicinal perspective, these recognition methods have low sensitivity to detect weak and complex edge structure which is necessary requirement in medical imaging. Although these techniques can be utilized in hybrid approach for extracting more robust results. [Figure 3.2](#) shows the results of sobel edge detector on test case image from DermQuest database [34].

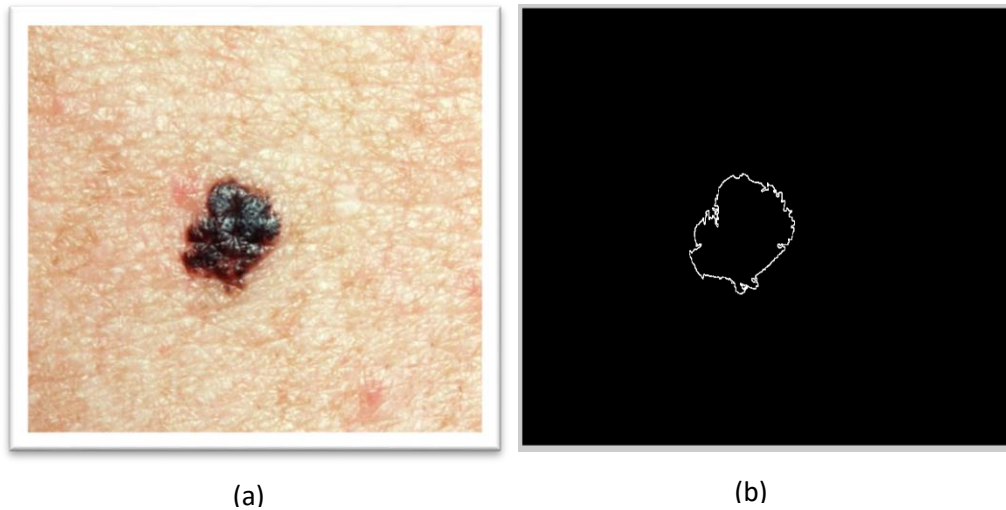


Figure 3.2: Sobel edge detector applied on test case image from DermQuest database [34] a) The original test case image, b) mole edges traced out using sobel edge detection method.

3.1.2.2 Canny Edge Detector

It is a multistage algorithm to detect more detailed edges from an image. There are five main steps of canny edge detector. In the first step, it smooth down the images by applying the gaussian filter. Secondly it computes the derivative of filtered images. An image actually has three main variables which includes x-coordinate, y-coordinate, and an intensity. So, by taking the derivative of an image brings it in two dimensions. We can take the derivative in the x direction and in the y direction, and together these make up the gradient vector. In the third step, it determines the magnitude and orientation of gradient. The fourth steps and fifth step applies the non-maximum suppression and hysteresis thresholding respectively to get the desired results. Non-maximum suppression suppresses the pixels which are not local maximum. Hysteresis thresholding works in the way that if the gradient at pixel is above high it declares it as the edge pixel whereas if the gradient at a pixel is below low it declares it as non-edge pixel. The fourth and fifth step of canny edge detector makes it superior as compared to sobel edge detector. Canny edge detector has good detection abilities. It is robust edge detection method and can perform well even with noise. It has good localization which means the edges detected are much closer to true edges of the image. One of the greatest advantage of canny edge detector is it gives single response constraint, which means it returns one point only for each edge point. [Figure 3.3](#)

shows the overall algorithmic approach of canny edge detector.

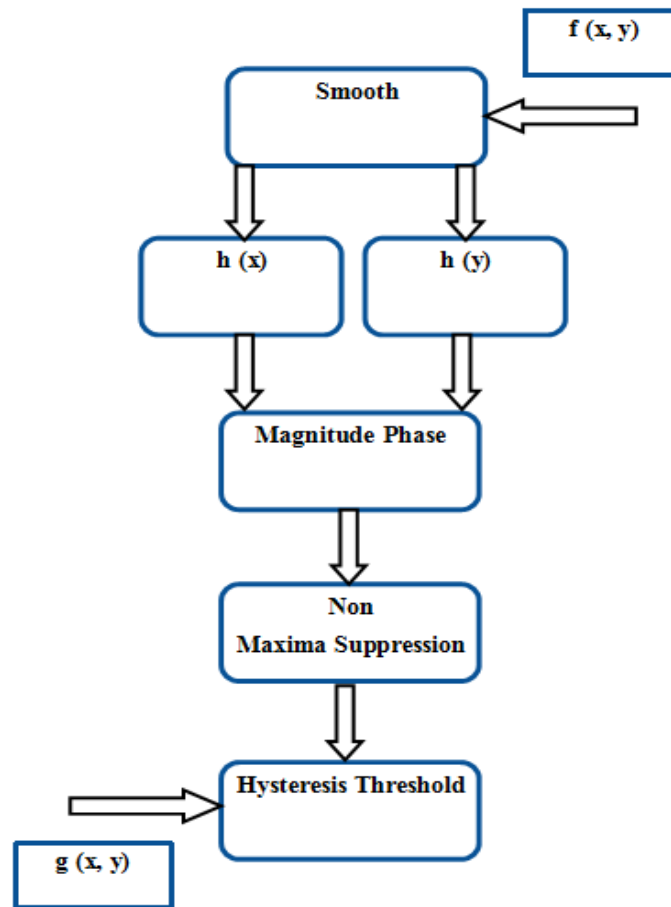


Figure 3.3: Overall algorithm of multistage canny edge detector with inputs $f(x, y)$ and outputs $g(x, y)$

3.1.3 Region Based Segmentation Techniques

Region based segmentation is another widely used image segmentation technique. This particular method of image segmentation works by identifying regions of some common property. For each pixel in the image we have to estimate to which class it belongs to. There are two main types of region segmentation algorithms which are as follows

- Region merging algorithms
- Region splitting algorithms

Region merging Algorithm: In region merging algorithm the neighboring regions/area are compared and merged if they meet the matching ratio in some property. Merging originates from uniform seed region. First method to perform region merging is to divide the image into 2×2 or 4×4 blocks and then check each one respectively. The second method

is to divide the entire image in to stripes. If the seed has been located its neighbors are merged until no more neighboring regions has uniform merging criteria [53].

Region Splitting Algorithms: In region splitting algorithm large non-uniform regions are broken in to small chunks which meets the uniformity. The process initiates from the entire image and divide it up until each small chunks of region are uniform. The main drawback of this algorithm is to decide where to make the partition [53].

The main advantages of region based segmentation techniques is it provide good results in noisy images where edges are of lighter intensity and hard to identify. But it has some disadvantages. Firstly, seed region must be defined or specified for the algorithm to work and secondly different seed points can provide different results which can eventually leads towards non-efficient segmentation technique. From medical point of view this segmentation technique is used in various medical applications like brain tumor diagnosis, MRI image segmentation, CT tumor detection.

3.1.4 Active Contours Method

Active contour (Snakes) or Deformable contour method is widely used image segmentation technique now a day for different applications. It can be defined as energy minimizing systems. The energy minimizing system are guided by external constraints forces and influenced by the image forces that pull it towards the features where image structure like boundary and edges exists. Active contour model lock onto nearby edge structure to localize them accurately. It is an iterative process which process iteratively to minimize the energy function which is shown in [Figure 3.4](#). In kass original model the total energy means the cost function of a snake can be represented by the following equation

$$E_{\text{Total}} = \int_0^1 (E_{\text{int}}(V(s)) + E_{\text{img}}(V(s)) + E_{\text{con}}(V(s))) \quad (1)$$

where $E_{\text{int}}(V(s))$ is the internal energy that encourages the prior shape preferences. E.g. image smoothness. $E_{\text{img}}(V(s))$ is the external image energy that forces the contour to fit around the boundaries of the object and $E_{\text{con}}(V(s))$ is the energy of contour [1].

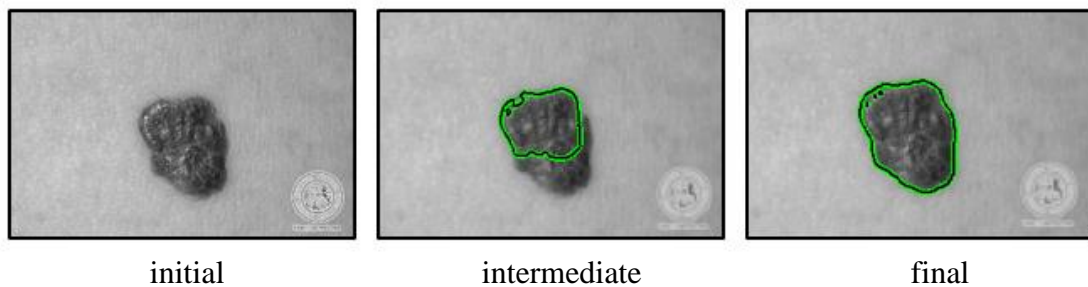


Figure 3.4: Active contour model iterative process to lock onto nearby edges of the lesion area by minimizing the cost energy function.

Vast progressions in medical imaging strategies and upcoming innovation stages have delivered a greater interest and enthusiasm of research group in the field of medical picture handling. The principal point is to enhance medical determination through precise segmented pictures. Techniques have been developed to help for identifying and diagnose specific structures within magnetic resonance images, computed tomography (CT) scan images, X ray images, malignant dermoscopic images and other such medical images. For all such type of medical imaging active contours models plays a vital role for precise and accurate segmentation. It is considered as one of the most successful technique and has achieved tremendous attention for locating and mapping complex boundary structures in medical images [6]. Skin cancer malignant mole segmentation is considered one of the most difficult task for dermatologists when performing manual segmentation and require years of practice. Active contour models can help and aid dermatologist for mapping complex malignant skin lesion structure to increase their diagnosis abilities which is reflected in [Figure 3.5](#) by applying active contour algorithm on test case image taken from DermQuest dataset [34]. The proposed research work for skin cancer mole segmentation focuses on active contours models which will be later discussed in chapter 5.

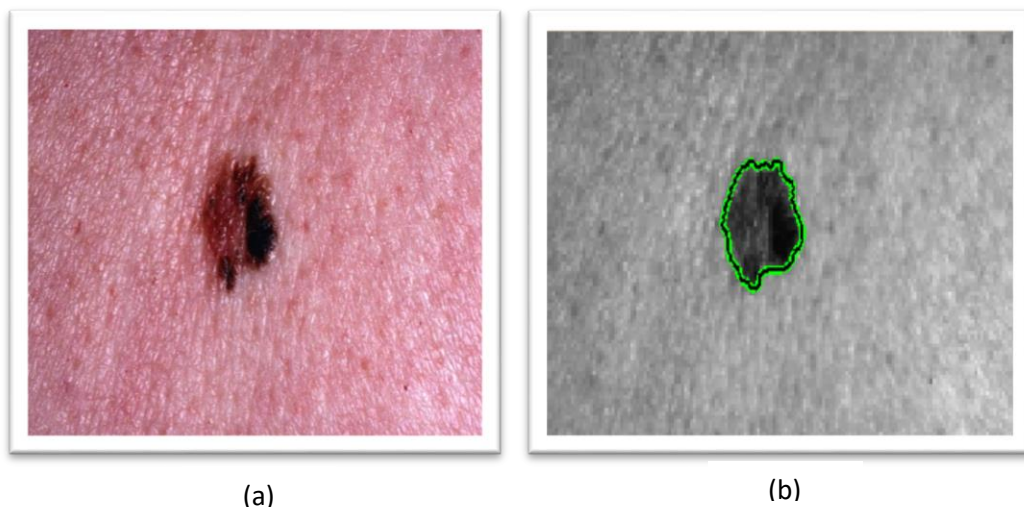


Figure 3.5: Active contour algorithm applied on test case image from DermQuest database [34] a) The original test case image, b) image converted to grayscale and lesion boundary segmented out using active contour method.

3.1.5 Watershed Segmentation

Watershed segmentation is considered as one of the finest and cutting edge segmentation technique for image boundary segmentation due to its precise and robust results. Watershed transform works by spreading out the drop of water following the gradient of the image which flows along the image path and finally detect the image boundary by reaching local minimum. As compared to active contours which is an iterative process), watershed is less

sensitive to noise and is less computationally expensive. Watershed algorithm is a type of topographical representation of gray level image displaying pixels in the form of valleys and hills where ‘valleys’ are brighter pixels and ‘hills’ are the darker pixels [2, 4, 21]. Each valley is associated with a catchments basin, and each point in the landscape belongs to exactly one unique basin which is shown in [Figure 3.6](#) [71].

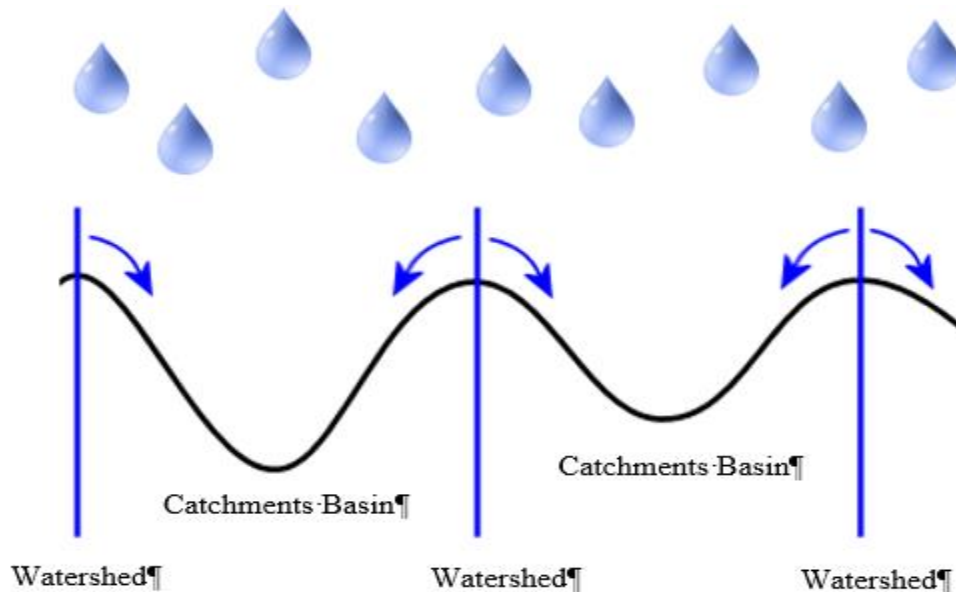


Figure 3.6: Watershed segmentation valley is associated with a catchments basin, and each point in the landscape belongs to exactly one unique basin [71].

Due to its robust and accurate results watershed segmentation is very useful and its performance is highly validated on medical images. It can perform rapid detection on both edges and boundary which is core requirement in medical imaging. It is widely used in different medical images like X ray images, CT scan images, dermoscopic images to diagnoses different diseases which includes cancer detection, brain tumor detection, and malignant skin lesion mole detection. Watershed transform is considered imperative segmentation technique for skin cancer mole detection and segmentation. It can help dermatologists to take guidance for accurate and precise segmentation of malignant mole which will ultimately help them for proper classification. The performance of watershed segmentation on one of the test case from Dermis database [33] is shown in [Figure 3.7](#). Along with precise and robust results of watershed segmentation there are also some disadvantages of this technique. For complex image structures watershed transform can generates over segmented results which can ultimately produce outputs with unwanted noise and local irregularities in gradient images. This problem can be avoided by reducing the number of minima and reducing the number of calculation of too many regions [8]. Secondly watershed method is highly sensitive to local minima, since at each minima, a watershed is created but this problem mainly occurs due to the noisy images. In that case,

it is recommended to either pre-process the image or it can be solved by adjusting sigma setting to smooth out the image [70].

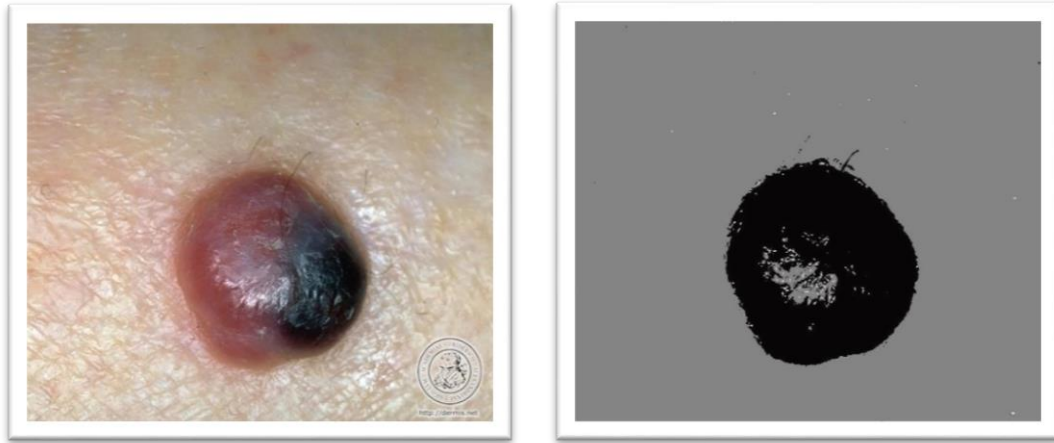


Figure 3.7: Watershed algorithm applied on test case image from Dermis database [33]
a) The original test case image, b) image converted to grayscale and lesion boundary and mole segmented out using watershed segmentation.

3.2 Advanced Segmentation Approaches

Merged segmentation and hybrid segmentation falls in the domain of advanced approaches often used in complex segmentation tasks especially in medical imaging. The idea behind such type of segmentation technique is to merge the results obtained from two or more segmentation techniques or use two segmentation approaches in parallel in order to increase the accuracy level of the segmented outputs. Such types of techniques are very useful in different medical imaging like magnetic resonance (MRI) imaging, computed tomography (CT) scan images, dermoscopic images as it makes the segmentation and detection process more rigid and robust. The proposed research work presents a novel segmentation technique for dermoscopic images formed by the merged approach of watershed segmentation and active contours method which will be later discussed in chapter 5. Other advanced segmentation techniques include fuzzy segmentation. Fuzzy algorithm works by assigning membership value to each pixel and if the membership are taken into account while calculating region properties we can obtain more accurate estimates of region properties [9]. The major advantages of advanced segmentation approaches is its high level accuracy which is highly preferable by research community and professionals.

Chapter 4

Skin Cancer Features Vectors and Classifiers Using Various Machine Learning Methods

This Chapter will particularly focus on advanced computer vision techniques for extracting different groups of features of lesion moles. After automated segmentation of malignant moles, the next step is feature extraction, which includes shape features, texture features, and color features. These features will be further used by a classifier system to differentiate between non-melanoma and melanoma cases. The next part of the chapter will present state-of-the-art classifiers based on machine learning and pattern recognition techniques for accurate and robust classification of malignant moles. It includes Support Vector Machines (SVM), Artificial Neural Networks (ANN), and deep learning methodologies which utilize Convolution Neural Networks (CNN).

4.1 Feature Vectors

Feature values play a vital and core role for classifying lesion areas. Feature vectors contain the numeric values which are obtained from different groups of features on the basis of which any classifier system can make an appropriate decision. In our proposed research work, we will be focusing on the ABCD clinical diagnosis method of dermoscopic images to classify between non-melanoma and melanoma cases. The ABCD method is a combination of four features for classifying between malignant melanoma and benign moles, which are abbreviated as ABCD where A stands for asymmetry of mole, B for border evolving, C for color variation, and D for diameter of the mole. Shape, texture, and color feature groups will collect a number of features which will be further used by state-of-the-art classifiers to estimate accurate outputs on the basis of the ABCD method of dermoscopy.

4.1.1 Shape Features

Shape features extract the information about the geometric structure of the overall segmented

mole which is also known as region of interest (ROI). By using the ABCD method of dermoscopy the most important shape feature is the symmetry of malignant area. According to which if the malignant mole is not symmetric either in one or both of axis then it is symbol of cancerous mole. Such type of moles is commonly known as asymmetric moles. The case under consideration is considered more critical if it is asymmetric from both of its axis. Shape features calculates the symmetry of lesion mole by estimating the center point and then drawing lines to both of the axis of the mole which will be further used to measure the symmetry of the mole. In the proposed research work we will work out three conventional shape feature from binary output of dermoscopic image which includes asymmetry, diameter of mole, compactness and ulnar variance. Compactness refers to the ratio of the object perimeter to its area. Ulnar variance is the measure of relative length of articular surfaces of some particular radius and the image asymmetry is the measure of asymmetry of the malignant mole. All of these features are computed in the form numeric values which are placed in shaped feature vectors.

4.1.2 Texture Features

It is another group of features which provide us the information about spatial arrangement of pixels or intensities in image. Texture features that may not be readily perceived by human eyes but it plays pivotal role for classifiers systems to effectively distinguish between normal skin and melanoma cancer lesion. In our proposed research work we have extracted texture features from binary and grayscale outputs of dermoscopic images. The texture features include coarseness and gray level co-occurrence matrix (GLCM). Gray level co-occurrence matrix features are extracted from gray level image. Coarseness can be defined as the measure of different angle texture representation. GLCM is a histogram of co-occurring grayscale values for given offset over the image and provides the feature discriminatory attributes. It consists of many different parameters which includes mean, correlation, homogeneity, contrast, energy, dissimilarity and kurtosis. Like shape features all of these features are also computed in the form of numeric values which are placed in texture feature vectors.

4.1.3 Color Features

Color features plays crucial role in clinical diagnosis. Using ABCD rule of dermoscopy Color features group extract information about the color variation of malignant mole which will be further used by the classifier system to classify between melanoma and non-melanoma case. Color features are gathered from RGB channel of dermoscopic image. For the proposed research the color related features include variance, skewness, and entropy. Variance is the measure of dispersion in the image. In medical imaging entropy is one of the most important color feature and it can be defined is the proportion of randomness. The third color feature includes skewness which is the measure of distributed asymmetry. After collecting all of the color features the numeric values are stored in color features vectors

4.2 Classifiers

Classifiers include a broad range of decision-theoretic approaches for the classification of wide range of images used in different applications. Classifier systems are based on assumptions approaches through which they make decisions. A good classifiers system mainly rely on good feature vectors to differentiate between different classes of image. In medical applications the classifiers play the core role for the diagnosis of different diseases. Image classification algorithm analyzes the numerical properties of various image features and organizes data into categories. Classification algorithms typically employ two phases of processing which are categorized as training and testing. In the initial training phase, characteristic properties of typical image features are isolated and, based on these, a unique description of each classification category, which is the training class, is created. In the subsequent testing phase, these feature-space partitions are used to classify image different group of features [63]. Some state of art classifiers includes support vectors machines (SVM), artificial neural classifiers (ANN) and deep learning methodologies.

4.2.1 Support Vector Machines (SVM)

Support vectors machines (SVM) is a type of supervised learning classifiers which is widely used in different machine learning applications. It is commonly used to classify between different classes and provide probabilistic results on the basis of its training data. It works by plotting each data item as a point in multi or n-dimensional spaces where n can be defined as possible number of features with the value of each feature as the value of a particular coordinate. Then in the next phase it perform characterization by finding the hyper-plane that is utilized to separate between the different classes extremely well [65]. Like any other classifiers support vector machine are based on decision planes that eventually defines its decision boundary.

As discussed above the main goal of Support Vector Machines is to calculate the optimal separating hyper plane which maximizes the training data. Mathematically it works by collecting the training data in the form of support vectors which lies on the margins .There are basically two main types of support vector machines which included linear soft margin support vector machines and nonlinear support vector machines. Linear SVM classifier separates a set of objects into their respective groups with a straight linear line also known as decision boundary but unfortunately most of the classification task are not that much simple and indeed they require complex classifier structures thus we use the non-linear SVM classifier. It makes decision on the desired test cases on the basis of the examples that are available in the training dataset [66].

4.2.2. Artificial Neural Networks (ANN)

Neural networks which is also known as connectionist computational system provides the best solution to complex problems in the field of image recognition. Artificial neural networks derives the concept of complex computations form human brain. The human brain can be described as biological neural network an interconnected web of more than 100 billons neurons transmitting elaborate pattern of minute power electrical signals. The overall structures contains three major layers which includes the input layer, hidden layer and output layer. Input layer also known as dendrites where input signals are received and after performing all its computations in hidden layers it provides us the desired output through output signal known as axon. In the same way artificial neural networks are designed which contains a number of neurons divided in to three main layers (input layer, hidden layer and output layer) that are interconnected with each other to perform computational task which is often referred to as pattern recognition. [Figure 4.1](#) shows the three main interconnected layer architecture of neural network.

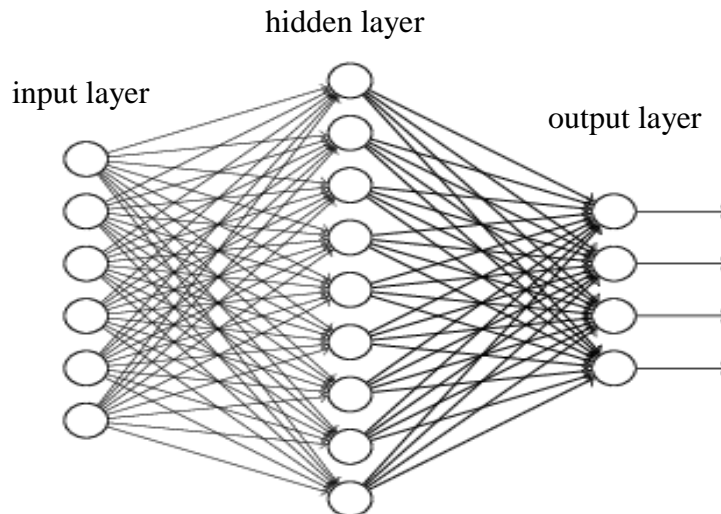


Figure 4.1: Neural network interconnected layers (input, hidden and output) architecture (Figure reprinted using noncommercial reprinting permission [49]).

Due to its quick adaptive learning ability on the basis of which it can change its internal state neural networks are widely in different computer vision application like face detection and recognition systems, automatic number plate recognition systems, a wide range of medical needs like tumor diagnosis system, lung cancer detection, skin cancer detection and other such pathologies. Mathematically a neural model works by adjusting the weights which can be defined as the connection between neurons. If the neural net generates good results weights are said to be adjusted but on the other hand if our neural net does not produce satisfactory results in the form of error signal then the system start altering the weights on the basis of its adaptive learning ability thus providing satisfactory outputs at one stage and finally draws the decision boundary [49]. Neural networks can work on three main learning techniques which include supervised learning, unsupervised learning and reinforcement learning which makes it more efficient and robust as compared to support

vector machines which only works on supervised learning method. In our proposed research work for skin cancer classification we have utilized neural network to classify between melanoma and non-melanoma cases on the basis of its feature value which will be later discussed in chapter 5.

4.2.3 Deep Learning Methods

Deep learning is an emerging area in the field of machine learning and it is has been introduced to achieve the goals of enhanced and improved classification accuracy level as compared to conventional neural classifiers. Deep learning methodologies play the vital role to achieve the major part in artificial intelligence. Normally the neural classifiers uses one or two hidden layers of neurons and they are most commonly used for supervised classification tasks but on the other hand deep neural classifiers architectures are entirely different from normal neural classifiers because they utilize more number of hidden layers which can range from three hidden layers to up till nine hidden layers which is shown in [Figure 4.2](#). Deep neural classifiers also differ form Support Vector Machines (SVM) as it can be trained using both supervised and unsupervised learning for their respective classifications tasks. Deep learning methodologies are used in wide range of applications which includes digital signal classification, image classification, and sound classification. Due to its precise and robust results these types of frameworks are widely used in complex image classifications which includes satellite imaging, medical image recognition, face recognition and other such type of tasks. The algorithms used for supervised deep leaning methodologies includes logistic regression, multilayer perceptron and deep convolution neural networks (CNN). The proposed research work will focus on Convolution Neural Networks (CNN) for skin cancer classification using digital dermoscopic images which will be later discussed in chapter 6.

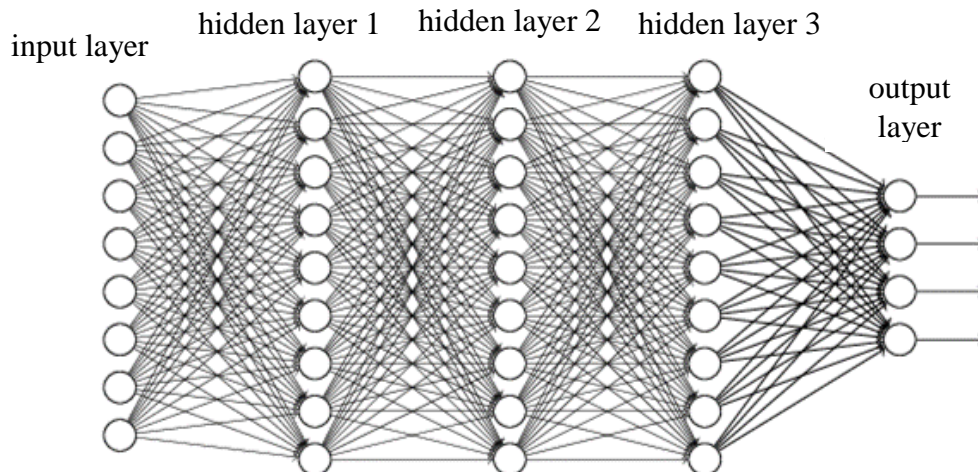


Figure 4.2: Three layer deep neural network interconnected layers (input, hidden and output) architecture (Figure reprinted using noncommercial reprinting permission [35]).

There are many open source deep learning libraries available which can be used to train and classify the images. These libraries are as follows

- Caffe developed by Berkeley Vision and Learning Center (BVLC) [26]
- TensorFlow by Google [67]
- Nvidia Digits by Nvidia Developers [50]
- Theano [68]
- MatConvent for Matlab [44]

All of these libraries are open sources and are based on parallel computing systems which means they can use the central processing unit (CPU) and graphical processing unit (GPU) together which will eventually improve the classification process to extreme levels. Tensorflow by Google utilizes its inception model which can be retrained to classify other classes of images. All of these libraries are designed to train and visualize the deep neural networks for wide range of image classification.

For the proposed research work two state of the art deep learning frameworks has been utilized which includes TensorFlow by Google brain and Nvidia Digits by Nvidia Developers which is later discussed in chapter 6.

Chapter 5

Proposed System Evaluation and Results

This chapter will focus on the major goals of this research work which is to design automated lesion detection system for correct mole segmentation and efficient classification process for correct diagnosis process between melanoma and other skin diseases or non-melanoma cases. This system will subsequently aid the dermatologist for taking correct decision. The contributions, test cases and results used in this chapter are published by me in IEEE BIBE 16th International conference Taiwan [10]. For more precise results two classifiers are used in parallel which includes Support Vector Machine (SVM) which is type of probabilistic classifier and Artificial Neural Network (ANN) which is type of non-probabilistic classifier. Once the results are extracted from support vector machines the desired case is also checked under neural classifier to reconfirm the results and to also check the results where support vector machines fails to classify the case under consideration. In the next phase, Deep Neural Networks (DNN) is applied on the proposed research work to increase classification accuracy in comparison with Artificial Neural Network (ANN) which is reflected in chapter 6. Later on, the obtained results are also confirmed with dermatologist results (ground truths) provided in datasets.

5.1 Datasets Used

As discussed above the main focus of the proposed research work is to develop a detection and classification framework which can illustrate the non-pigmented skin malignancies along with the pigmented skin growth. The test datasets utilized for this work is collected from three databases which includes PH², DermIS and DermQuest. The complete details of these datasets is given in [Table 5.1](#). All of the datasets used for the proposed research are freely available on open Internet. Whereas paid datasets are also available for academic and medical research purposes. One of the paid datasets includes Dermofit Image Library [36]. This dataset is composed of a total of 1300 skin images with corresponding class labels and lesion segmentations.

TABLE 5.1: Dataset

Dataset Details		
S.NO	Dataset	Attributes
1	PH ² [15, 32]	This database is obtained from Dermatology Service of Hospital, Pedro Hispano (Matosinhos, Portugal) known as PH ² [15]. The PH ² database is based on the process of manual segmentation, the clinical diagnosis, and the identification of several dermoscopic structures which is performed by professional dermatologists. It contains a total of 200 hundred images which include both melanoma and non-melanoma cases. All the images in this dataset are taken under the same conditions through Tuebinger Mole Analyzer system using a magnification of 20x.
2	DermIS Database [33]	Dermatology Information System also known as DermIS is developed by the cooperation of University of Heidelberg (Dept. of Clinical Social Medicine) and University of Erlangen (Dept. of Dermatology) [33]. DermIS.net is the largest dermatology information service available on the internet. It offer elaborate image atlases (DOIA and PeDOIA) complete with diagnoses and differential diagnoses, case reports and additional information on almost all skin diseases including skin cancer.
3	DermQuest Database [34]	DermQuest is also one of the largest dermatology information service available on the internet. For dermatologists and healthcare professionals with an interest in dermatology. The overall database contains extensive range of clinical image library which contains the images shared by wider dermatology community which includes skin diseases images along with skin cancer images. Moreover, it also has interactive dermatology-specific learning Modules, which provide access to continued learning. This database is available for dermatologist with greater interests in patient practice and for academic research.

5.2 Proposed Algorithm/ Approach

In the proposed research work cancerous mole evaluation and classification system has been implemented for the detection of malignant melanoma (skin cancer mole) on any part of body. The proposed algorithm for this research work is shown in Figure 5.1 [10].

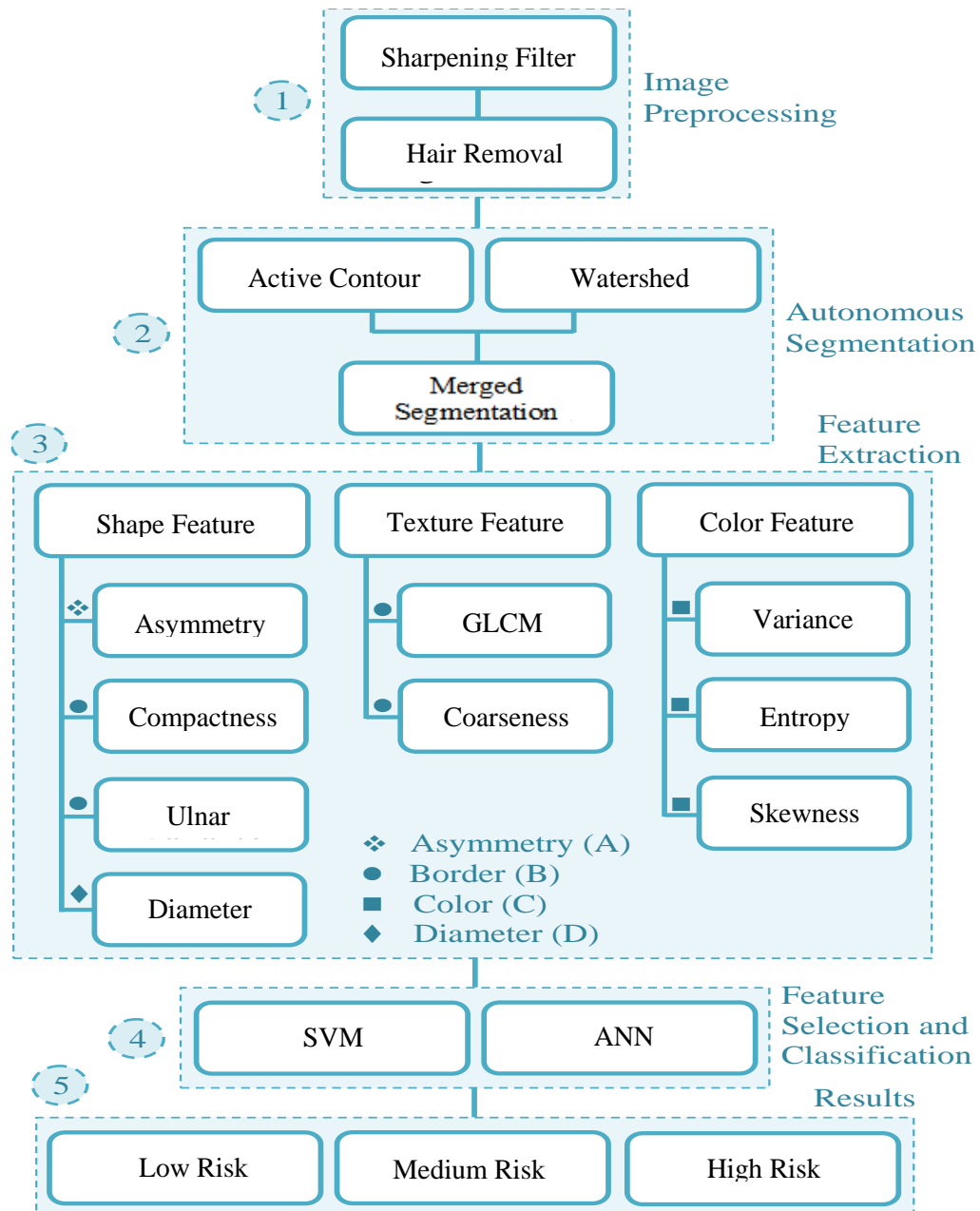


Figure 5.1: Proposed algorithm of the overall automatic lesion detection system (ALDS) for skin cancer classification

The algorithm consists of five steps starting from the input phase of preprocessing the dermoscopic images ranging to the analysis in the form of likelihood of Lesion Malignancy for the desired case.

5.2.1 Preprocessing of Digital Dermoscopic Images

It includes the process of acquiring the images of the required area. In our case, we are using PH² [32, 15] database. All the images have resolution of 765x573 pixels and it contains a total of 200 images including both melanoma and non-melanoma cases. Moreover, we have also used the dataset from DermIS [33] and DermQuest [34]. These datasets contain both melanoma and non-melanoma images of different resolutions. i.e. 550x451, 550x469, 550x367 etc. Images are refined by applying a initial sharpening filter and hair removal process using dull razor software [14] has been applied for removing clutter [10].

5.2.2 Autonomous Segmentation of the Cancer Mole

This phase segments out the cancerous mole autonomously. The segmented region plays an important role to calculate certain features required for further analysis. We have used the merged approach/response of active contour and watershed algorithms for segmentation. Active contours help to learn the point distribution model while watershed helps identify the closed contour. Their individual performance varies and at times goes low in complex cases. The same has been verified through the similarity measures using different measurement parameters which includes structural similarity index (SSIM), jaccard coefficient and dice coefficient computed in the Section IV of this chapter. Combining these techniques essentially helps to crop the desired region that nearly match the ground truth segmented masks provided in the datasets [10].

Watershed Algorithm: Watershed Algorithm is one of the most efficient and successful region based segmentation techniques used for segmentation especially in the field of medical imaging. As compared to active contours (an iterative process), watershed is less sensitive to noise and is less computationally expensive. Watershed algorithm is a type of topographical representation displaying pixels in the form of valleys and hills where ‘valleys’ are brighter pixels and ‘hills’ are the darker pixels [2, 4, 21]. In our case we are using it to segment out the skin cancer mole as it has the ability to efficiently track even weak boundary areas of lesion mole. After extraction, the boundary is smoothed out by means of zero padding and binary image morphological operation so as to obtain final mask of skin cancer mole.

Active Contour: It is a region segmentation technique and is defined as an energy minimizing spline used to locate the object where image structures, such as boundaries exists [23]. It is an iterative process that works to minimize the energy function. As

discussed in chapter 3 section 3.2.4 in kass original model the total energy means the cost function of a snake can be represented by the following equation

$$E_{\text{Total}} = \int_0^1 (E_{\text{int}}(V(s)) + E_{\text{img}}(V(s)) + E_{\text{con}}(V(s))) \quad (1)$$

where $E_{\text{int}}(V(s))$ is the internal energy that encourages the prior shape preferences. E.g. image smoothness. $E_{\text{img}}(V(s))$ is the external image energy that forces the contour to fit around the boundaries of the object and $E_{\text{con}}(V(s))$ is the energy of contour [1].

5.2.3 Merged Segmentation Results

In our initial findings, the results were not consistent when individual binary masks were used, which led us to merge the masks obtained from active contour and watershed. It is performed by subtracting the watershed segmented image from active contour part which is then complemented and finally the resulting image is multiplied to watershed segmented image. The resulted merged mask then undergoes certain morphological operations like image dilation and image spur for removing spur pixels to get the smoothness and the boundary continuity. As a result, the final mask contains the exact boundary and the necessary surrounding area of the skin lesion, which is not obtained by either mask separately [10].

5.2.4 Similarity Measures

Once the merged results are obtained, the similarity measure is computed with reference to the ground truth provided in the dataset. This is done by calculating the Structural Similarity Index (SSIM) [64], Jaccard coefficient [43] and Sorenson Dice coefficient [60] of the computed mask and the ground truth mask provided in the dataset. These coefficients are widely used for the matching purpose and provide better quantitative insight to the change in structural information [10].

Structural Similarity Index (SSIM): The SSIM is defined by the equation.

$$\text{SSIM}(x, y) = \frac{(2\mu_x\mu_y + c_1)(2\sigma_{xy} + c_2)}{(\mu_x^2 + \mu_y^2 + c_1)(\sigma_x^2 + \sigma_y^2 + c_2)} \times 100 \quad (2)$$

where μ_x , μ_y , σ_x , σ_y , and σ_{xy} are the local means, standard deviations and the cross covariance of the two image objects x and y and c_1 and c_2 are some index parameters.

Jaccard coefficient: On the other hand, the Jaccard coefficient is a common technique to find the similarity index between the binary variables. It is defined as the intersection and union quotient of the pairwise compared variables between two different binary objects [10].

$$d^{JAS} = \frac{a}{a + b + c} \times 100 \quad (3)$$

Where d^{JAS} is a symbol of Jaccard coefficient, a is the number of common variables in both objects, b is the number of unique variables in first object and c is the number of unique variables in second object.

Sorenson Dice coefficient: Similarly, the Sorenson-Dice coefficient is also a similarity measure approach [10] defined as

$$d(A, B) = \frac{2|A \cap B|}{|A| + |B|} \times 100 \quad (4)$$

where A and B are the unique variables in object A and B .

5.2.5 Feature Extraction

This part of algorithm computes the features related to shape, texture and color from the segment mole. Using these three features categories, this approach collects ABCD data of lesion mole where A defines the asymmetry, B corresponds to border Evolving, C is related to color variation and D is the diameter of the mole. These features are represented with \diamond , \blacklozenge , \blacksquare , \bullet symbols respectively in Figure 5.1. The shape features includes image diameter, image compactness, ulnar variance and the image asymmetry. Compactness refers to the ratio of the object perimeter to its area. Ulnar variance is the measure of relative length of articular surfaces of some particular radius and the image asymmetry is the measure of asymmetry of the cancerous mole. The texture features include coarseness and Gray Level Co-occurrence Matrix (GLCM). Coarseness is the measure of different angle texture representation. GLCM is a histogram of co-occurring grayscale values for given offset over the image and provides the feature discriminatory attributes. It consists of different parameter which includes mean, correlation, homogeneity, contrast, energy, dissimilarity and kurtosis. The color related features include variance, skewness, and entropy. Variance is the measure of dispersion in the image. Entropy is the proportion of randomness and skewness is the measure of distributed asymmetry [10].

5.2.6 Feature Selection and Classification

This phase utilizes supervised learning techniques. i.e. Support Vector Machines (SVM) and the Artificial Neural Networks (ANN). SVM assign weights to all the selected features excluding diameter as it will vary for each test image. A total combination of 73 conventional features were selected from shape, texture and color features group. The first three features were extracted from shape features group which includes asymmetry, image compactness and ulnar variance. From the texture group 46 features were extracted among which 44 were selected from gray level co-occurring matrix (GLCM) and 2 from coarseness. Remaining 24 features were selected from color feature group in the form

of 8 variance, 8 entropy and 8 skewness features. The feature having smallest weight is considered as the least informative feature and eventually gets rejected. This elimination process iterates till all the outliers are eliminated. Hence, SVM comes up with the best features that are utilized for further mole analysis. Once good features are selected, SVMs is used to differentiate between melanoma and non-melanoma images. Further to improve system performance, ANN classifier is used as a second level classifier to reevaluate the results obtained from SVM and to classify the cases where SVM fails i.e indeterminate cases. The ANN classifier uses eight feature inputs that include mean, correlation, homogeneity, contrast, energy, kurtosis, dissimilarity and skewness. There are ten hidden neurons and one output neuron. Neural Classifier is trained by applying back propagation algorithm by providing the eight feature values of each case in input matrix and desired outputs is stored in the target matrix [10].

5.2.7 Results

This Last phase of the overall algorithm is classifying the segmented mole on the malignancy probability using support vector machines (SVM) and number of cancerous condition matched using the artificial neural classifiers (ANN). It is the most important part that helps the physicians and dermatologist to diagnosis the case under consideration. SVM generates the results in the form of high risk which means it is melanoma case, low risk which means it is non-melanoma and medium level risk which means it is an indeterminate case. Indeterminate cases can be further classify by using ANN classifiers whereas ANN classify can also be used to revalidate the results obtained from SVM and if the dermatologists still remain confused the desired case can be diagnosed by performing the biopsy test [10]. The probalistic results generated from SVM as given in [3] can be calculated as

$$P = 2 * (F - \min) / (\max - \min) - 1 \quad (5)$$

(Where F = Image feature vector, min = Minimum feature values of cancerous area, max = Maximum feature values).

5.3 Software Used

The proposed algorithm has been implemented using Matlab R2013B ® and tested on the Intel Core i5 based computing platform. Though it can also run on Matlab R2014 ® and next versions. The whole process of classification takes approximately up to 4 minutes and generates the final results.

5.4 Test Cases and Graphical User Interface (GUI)

The proposed algorithm was tested on different classes of dermoscopic images from the datasets as described in chapter 5 section 5.1 among which certain were selected for the proposed research work which are shown in [Figure 5.2](#) accordingly [10].

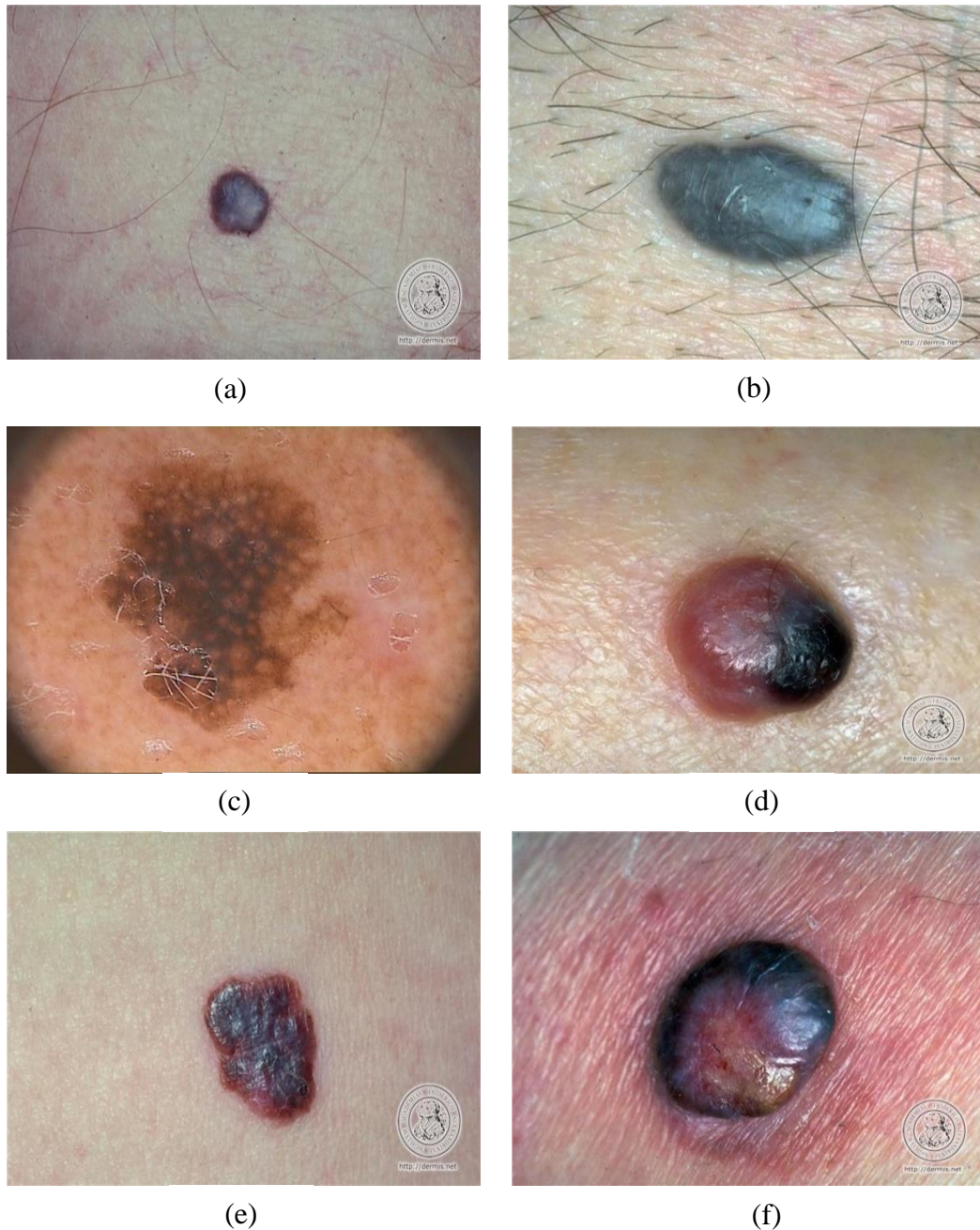


Figure 5.2: Test cases for the proposed research work for which binary mask will be segmented and classification results will be generated

It is to be noted that the available datasets have images taken in controlled illumination and pose. Any variation in these parameters is expected to affect these results. Such an example is shown in [Figure 5.3](#).

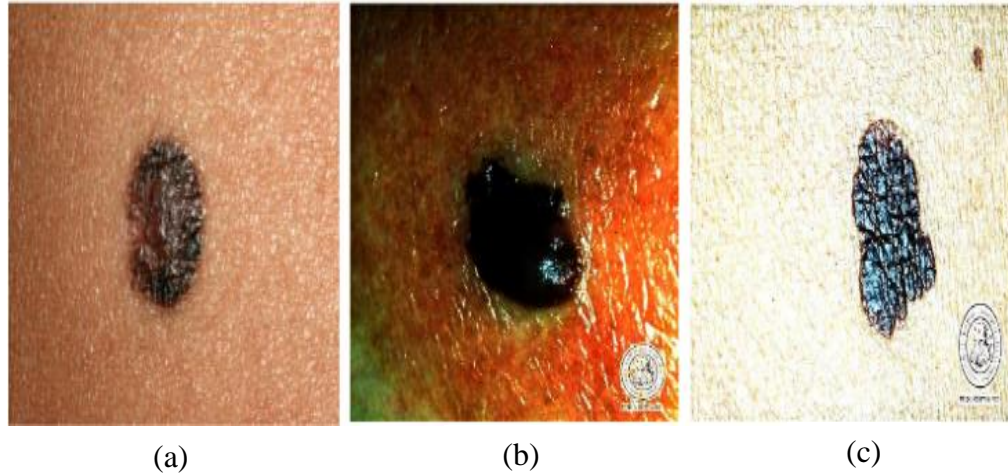
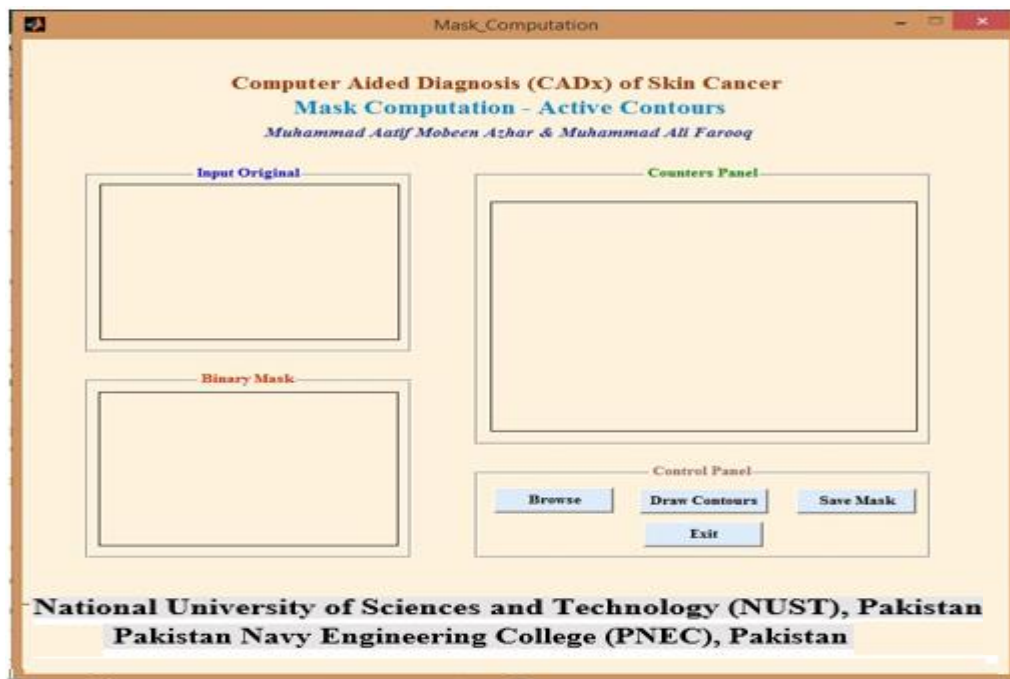
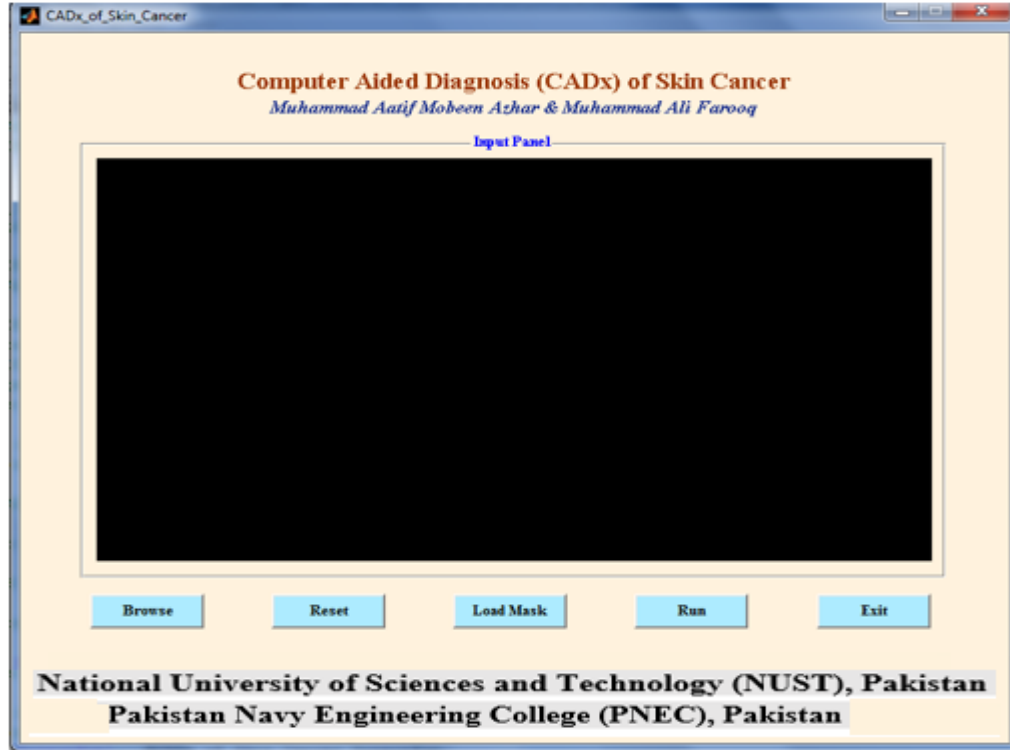


Figure 5.3: Images under changed lightning conditions a) good lightning conditions b) & c) inappropriate lighting condition,

Graphical user interface (GUI) has been designed for computing the active contour mask and main evaluation for classifying the case under consideration which are shown in [Figure 5.4](#) accordingly



(a)



(b)

Figure 5.4: GUI for the proposed research work, a) active contour GUI, b) main evaluation GUI

5.5 Merged Approach for Binary Mask Computation

This step consists of the segmentation task, in which the cancerous area is segmented. The watershed algorithm provides the segmentation results as shown in [Figure 5.5](#). The active contour iterative process provides the segmentation results as shown in [Figure 5.6](#). The overall all process of watershed and active contour merged approach is separately shown in [Figure 5.7](#). The masks computed for all the test images using watershed, active contour and merging both techniques along with the ground truth are shown in [Figure 5.8](#).

The watershed algorithm is applied to all the test images as shown in [Figure 5.2](#). It includes five main steps to finally produce the refined results which includes applying initial watershed algorithm, in the next phase we apply filtering to initial watershed results, then we perform border cleaning and border sampling steps and in the last phase we apply the final smoothing to overall binary segmented outputs. The whole process is shown in [Figure 5.5](#) accordingly [10].

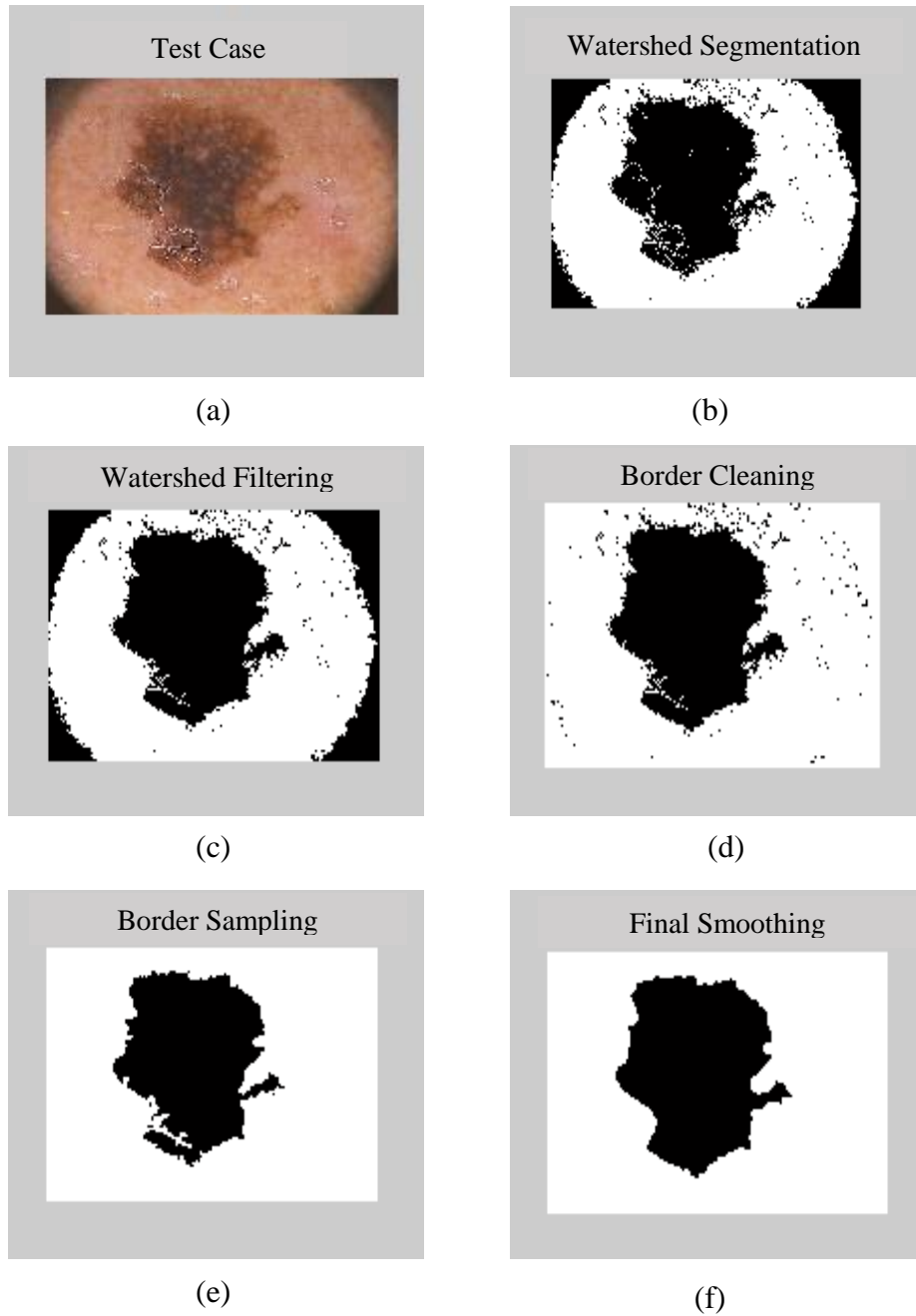


Figure 5.5: Overall watershed algorithm process applied to test case (b) of Fig 5.2

After producing the watershed mask the step is to compute the active contour binary mask. As discussed in [section 5.2.2](#) of chapter active contour is an energy minimizing spline and it is an iterative process. In our proposed algorithm, the active contour iterates 1000 times to produce final segmented binary outputs which is shown in [Figure 5.6](#)

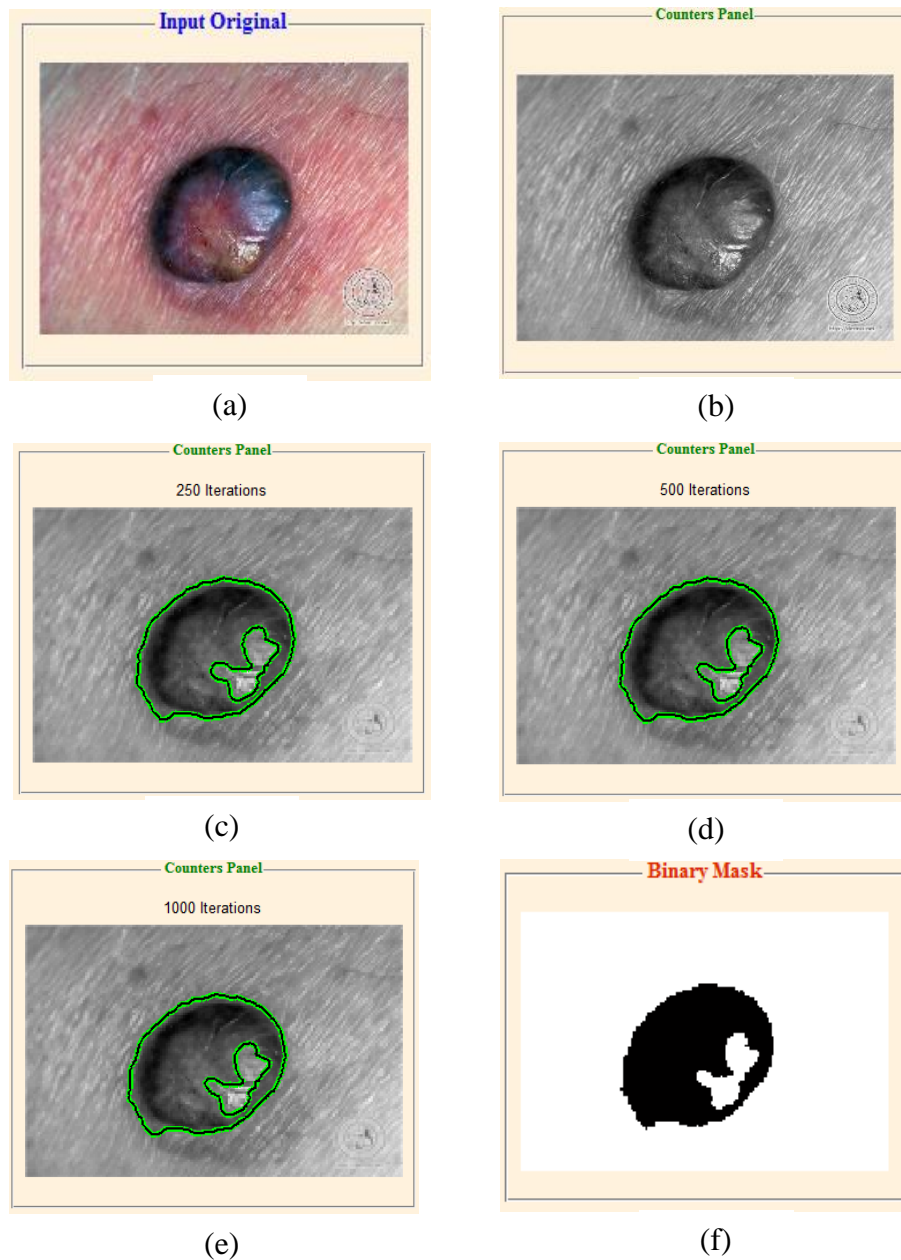


Figure 5.6: Overall active contour iterative process a) process applied to test case (f) of Fig 5.3, b) the image is converted to gray scale image, c) the process iterates for 250 times, d) the process iterates for 500 times, e) the process iterates for 1000 times, f) after 1000 iterations final active contour binary mask is generated

After producing the watershed mask and active contour mask the next phase is to generate the merged mask using the final outputs of watershed and active contour mask. It is performed by subtracting the watershed segmented image from active contour part which is then complemented and finally the resulting image is multiplied to watershed segmented image. The resulted merged mask then undergoes certain morphological operations like

image dilation and image spur for removing spur pixels to get the smoothness and the boundary continuity. As a result, the final mask contains the exact boundary and the necessary surrounding area of the skin lesion, which is not obtained by either mask separately. The complete process of merged approach is shown in [Figure 5.7](#) [10].

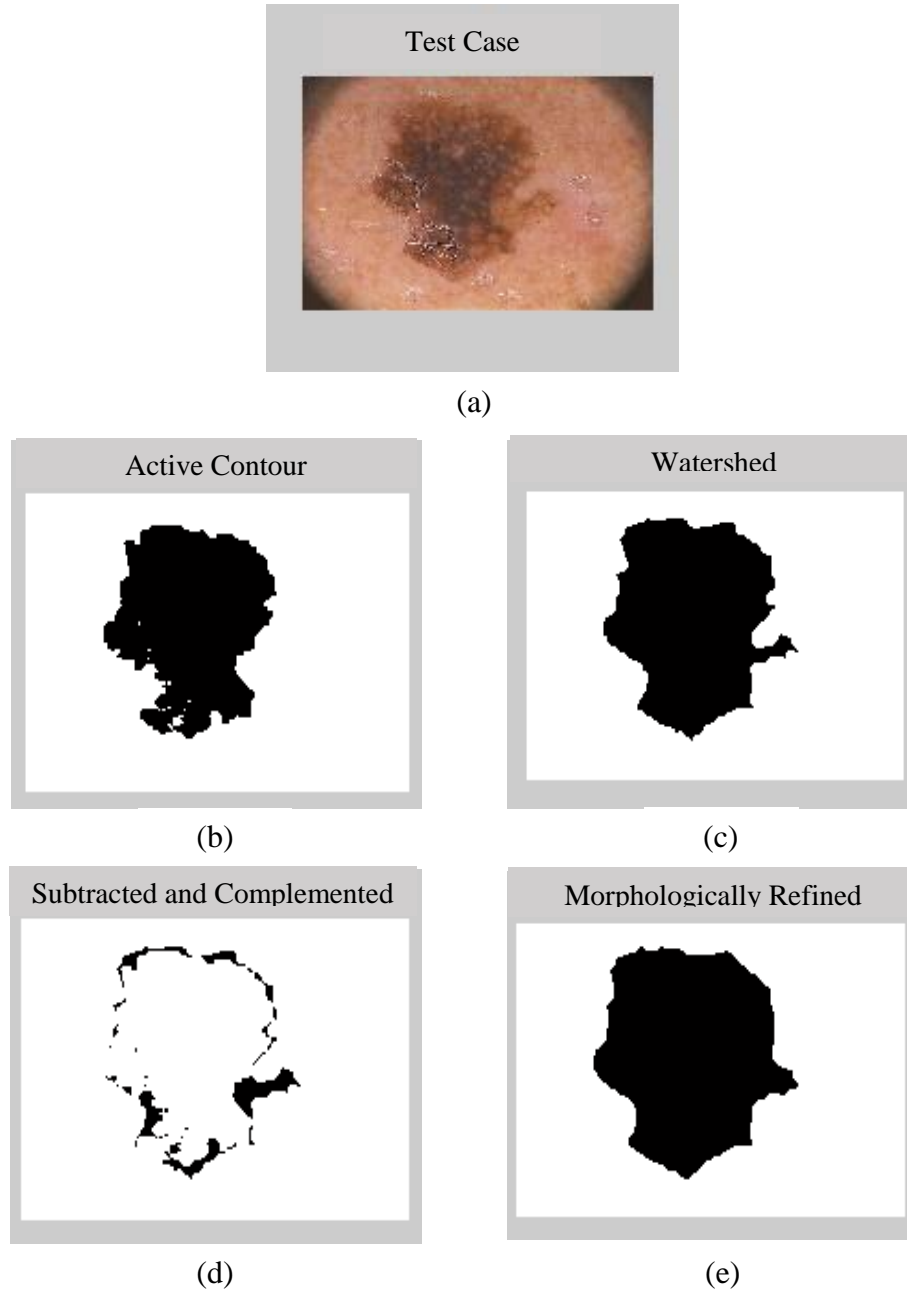


Figure 5.7: Overall detailed merged process using individual watershed and active contour binary mask applied to test case (b) of Fig 5.2

The merged approach of active contour and watershed algorithm is applied to all the test cases which is shown in Figure 5.8 accordingly along with their original binary mask provided in the dataset [10].

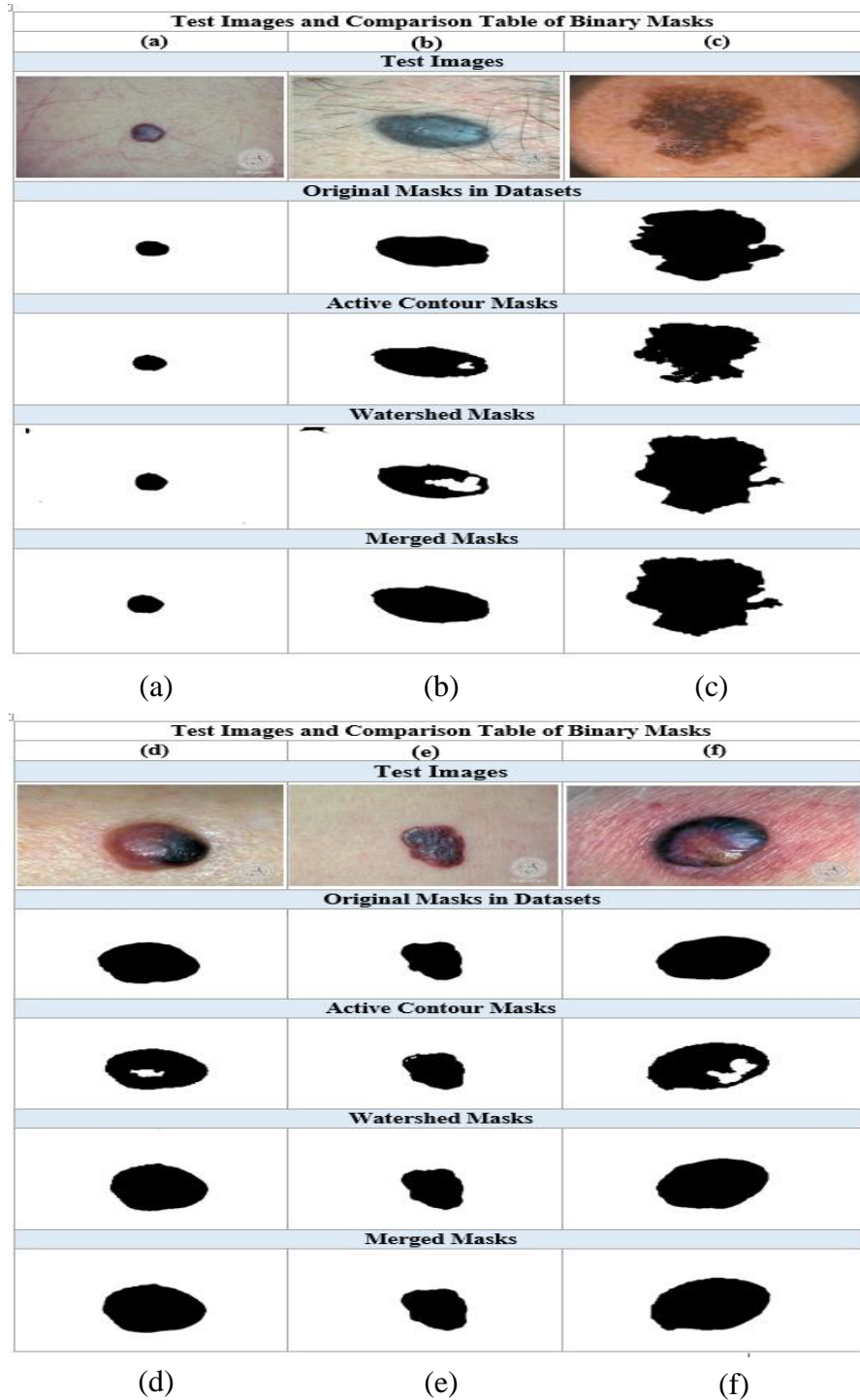


Figure 5.8: Test images along with their original mask, active contour mask, watershed mask and merged mask (Dataset [32-34])

5.6 Results

After binary mask segmentation using the merged approach of watershed and active contour algorithm the next phase is to compute the results which are divided in two main parts which are as follows

- Binary mask similarity results from ground truth
- Classification Results

5.6.1 Binary Mask Similarity Results from ground truth

The binary mask similarity measure is calculated by comparing each computed mask obtain through watershed technique, active contour method and merged approached which is respectively shown in [Figure 5.8](#) for all the test cases with the ground truth mask. The results of Structural Similarity Index (SSIM), Jaccard's coefficient and Sorenson-Dice coefficient [10] are provided in [Table 5.2](#)

TABLE 5.2: Binary Mask Similarity Results

Images	Active Contour Mask & Original Mask	Watershed Mask & Original Mask	Merged / Intersected Mask & Original Mask
Structural Similarity Index (%)			
Fig. 5.8 (a)	99.7	99.6	99.8
Fig. 5.8 (b)	99.8	99.6	99.9
Fig. 5.8 (c)	98.9	99.1	99.6
Fig. 5.8 (d)	99.8	99.8	99.9
Fig. 5.8 (e)	99.95	99.92	99.96
Fig. 5.8 (f)	99.37	99.65	99.72
Jaccard Coefficient (%)			
Fig. 5.8 (a)	99.7	99.7	99.85
Fig. 5.8 (b)	98.3	96.5	99.16
Fig. 5.8 (c)	89.6	93	95.8
Fig. 5.8 (d)	98.3	98.5	99.1
Fig. 5.8 (e)	99.5	99.3	99.6
Fig. 5.8 (f)	94.48	96.7	97.42

Images	Active Contour Mask & Original Mask	Watershed Mask & Original Mask	Merged / Intersected Mask & Original Mask
Sorenson Dice Coefficient (%)			
Fig. 5.8 (a)	99	99.2	99.85
Fig. 5.8 (b)	99	98.2	99.6
Fig. 5.8 (c)	94.5	96	97.9
Fig. 5.8 (d)	99.1	99.3	99.5
Fig. 5.8 (e)	99.7	99.6	99.8
Fig. 5.8 (f)	97.16	98.14	98.69

5.6.2 Classification Results

Once the lesion mole has been segmented out the mask is loaded on actual RGB image shown in [Figure 5.9](#). The next step is to evaluate the mole. SVM classify the result in form of either Low risk i.e. non-melanoma, Medium risk i.e. indeterminate or High risk i.e. melanoma. This is done by computing the necessary features and the probability percentage (eq. 5) as discussed in [section 5.2.7](#). However, SVM may provide varying results depending upon the skewed or imbalanced datasets and often classify the case in the form of medium level risk i.e. indeterminate case. Therefore, Artificial Neural Networks (ANN) are also used in a complementary role [10].

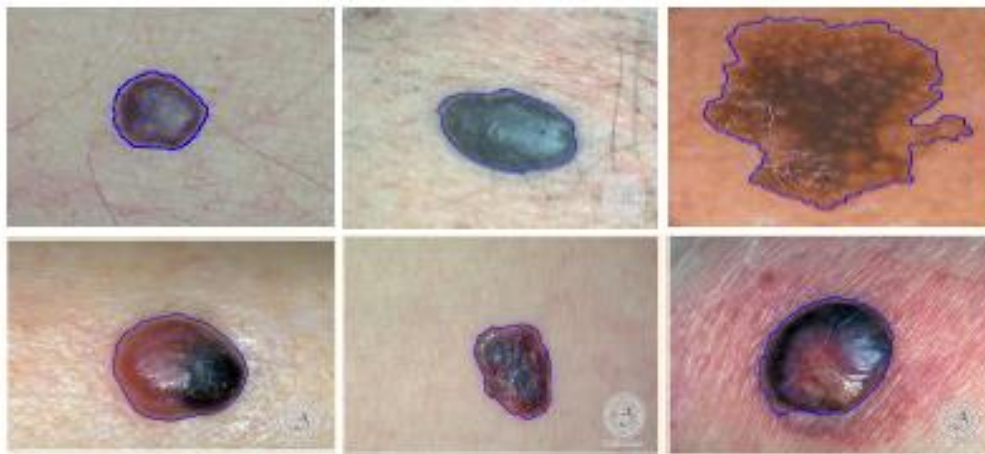
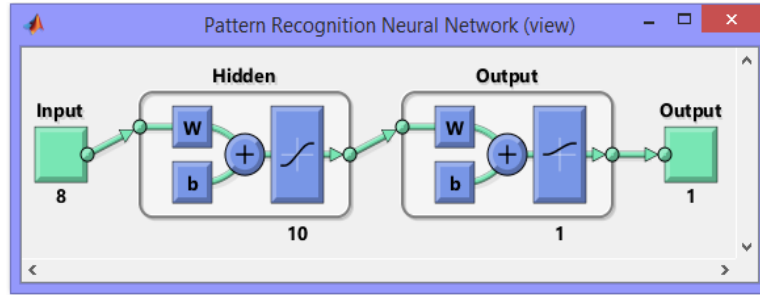


Figure 5.9: Six different cases of different categories with masks loaded on actual test images.

ANN classifies the mole in the form of zero (Low risk) and one (High risk) where one indicates melanoma (cancerous) mole and zero indicates non melanoma mole. The ANN classifier is trained using both melanoma and non-melanoma cases. The results contain six misclassification and accuracy of the system is 80% as compared to dermatologist's findings. The neural network confusion matrix and ROC [10] are shown [Figure 5.10](#).

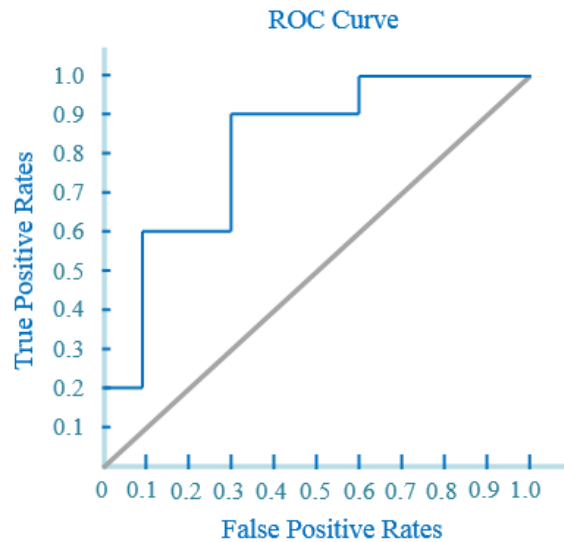


(a)

Confusion Matrix with 80 % accuracy

	0	1	
0	11 36.7 %	2 6.7 %	84.6 % 15.4 %
1	4 13.3 %	13 43.3 %	76.5 % 23.5 %
	73.3 % 26.7 %	86.7 % 13.3 %	80.0 % 20.0 %
	0	1	
	Target Class		

(b)



(c)

Figure 5.10: Artificial neural classifier, a) overall neural network with 10 hidden neurons, b) confusion matrix with 80% accuracy rate, c) ROC curve

The classification rule for SVMs and for Neural Classifier is provided in [Table 5.3](#). The classification results based on these rule are shown in [Table 5.4](#) and [Table 5.5](#) respectively which shows that the dataset images of [Figure 5.8 \(a\)](#) and [\(b\)](#) have the low probability (i.e. $< 50\%$) of becoming melanoma and hence are classified as low risk level. Similarly, the image of [Figure 5.8 \(c\)](#), [\(d\)](#) and [\(f\)](#) has the greater probability (i.e. $\geq 50\%$) hence, it is classified as high risk level which means that it is a melanoma case. Whereas [Figure 5.8](#)

(e) have medium level risk using SVM which was further classified using ANN and diagnosed as high level risk. These results also match ground truth provided within databases [39].

TABLE 5.3: Classification Rules

For SVM	
Probability > 0.40	Risk Level: High
Probability > 0.30	Risk Level: Medium
Probability < 0.30	Risk Level: Low
For Neural Classifier	
Matching Probability \geq 50%	Risk Level: High (Output 1)
Matching Probability < 50%	Risk Level: Low (Output 0)

TABLE 5.4: Classification Results using SVMs

SVMs Results			
Image	Probability (%age) with Original Mask	Probability (%age) with *Merged Mask	Classification
Fig. 5.8 (a)	16.2	19.4	Risk Level: Low
Fig. 5.8 (b)	18.7	21.7	Risk Level: Low
Fig. 5.8 (c)	58.4	51.5	Risk Level: High
Fig. 5.8 (d)	40.5	46.5	Risk Level: High
Fig. 5.8 (e)	33.1	32.3	Risk Level: Medium
Fig. 5.8 (f)	77.0	75.8	Risk Level: High

TABLE 5.5: Classification Results using Neural Classifiers

Neural Classifier Results	
Image	Classification
Figure 5.8 (a)	0 (Risk Level: Low)
Figure 5.8 (b)	0 (Risk Level: Low)
Figure 5.8 (c)	1 (Risk Level: High)
Figure 5.8 (d)	1 (Risk Level: High)
Figure 5.8 (e)	1 (Risk Level: High)
Figure 5.8 (f)	1 (Risk Level: High)

5.7 Quantitative Comparison of Diagnostic Results with Published Systems

The below table shows the comparison for accuracy level and state of the art algorithms used between the proposed work and other published systems which are shown in below table. These systems utilize the different of clinical diagnosis technique as the proposed system utilizes the ABCD method of dermoscopy. The proposed system details are bold and mentioned in last row of table. It should be noted that proposed system uses four state of art algorithms for segmentation and classification task and archives the upright accuracy levels.

TABLE 5.6.: Quantitative Comparison table of published system with proposed system

S.no	Paper Title	Medical Imaging Category	Area Of Interest	Algorithm's Applied	Accuracy
1.	A Combined Segmentation Approach for Melanoma Skin Cancer Diagnosis [19]	Dermoscopic images	Lesion Detection	Median filtering and active contour methods	-

2.	Nuclear Segmentation For Skin Cancer Diagnosis From Histopathological Images [17]	Histopathological Images	Segmentation and Classification	C- means algorithm and neural classifiers	
3.	SVM based Texture Classification and Application to Early Melanoma Detection [22]	Dermoscopic images	Classification	Support Vector Machines (SVM)	70 %
4	Computer aided Diagnosis of Melanoma Using Border and Wavelet-based Texture Analysis [11]	Dermoscopic images	Classification	Support Vector Machines and Logistics model tree	91 %
5	Set Of Descriptors For Skin Cancer Diagnosis Using Non-Dermoscopic Color Images [13]	Non-Dermoscopic Images	Classification	Artificial Neural Networks (ANN)	76 %
6	Automatic lesion detection System for Skin Cancer Classification Using SVM and Neural Classifiers [10]	Dermoscopic Images	Segmentation and Classification	Active contours, Watershed algorithm Support Vector Machines (SVM), Artificial Neural Networks (ANN)	80 %

5.8 Advantages of Proposed Research work

Following are some of the advantages of the proposed research work

- Technology advanced platforms minimizes the chances of error and false indications
- More computational power with improved techniques and algorithms of artificial intelligence makes it reliable and robust for complex classification cases.
- High sensitivity and improved accuracy for robust performance.

5.9 Challenges of Proposed Research work

Following are the some of the challenges of the proposed research work.

- Diagnosis and classification between diversified skin diseases other than cancer
- Varying illumination conditions and slightly varying pose of the region of interest can cause problems for mole segmentation and classification systems
- Evolving part of ABCDE method is difficult to work out because such type of datasets with picture of same cases progress over time are not available.

Chapter 6

Deep Learning Methodologies for Skin Cancer Classification

This chapter will focus on deep learning methods for skin cancer classification. Deep learning is an emerging field now a day which has been introduced with primary role of moving machine learning much closer to one of its original goal which is to achieve high classification accuracy levels. It is widely used in different applications because of its precise and accurate results as compared to other conventional classifiers. For the proposed research work we have used two major deep learning libraries for skin cancer classification which include TensorFlow™ by Google and Nvidia Digits library by Nvidia. The results have been computed on different test cases after retraining different state of the art models.

6.1 Datasets Used

For the proposed research same datasets have been utilized which were discussed in chapter 5 section 5.1 which includes Dermis, DermQuest and PH². For the training purpose different RGB images have been selected from these datasets and after successful training of classifiers the results were being tested on different images which were also selected from these datasets.

6.2 Deep Learning Libraries Used

For the proposed research work we have utilized two state of the art deep learning libraries which includes TensorFlow™ by Google [67] and NVIDIA DIGITS library by NVIDIA [50]. These libraries are open source and can be used for both research purpose and production environment. Both of these libraries includes pre-trained models which can be retrained for custom classification tasks. TensorFlow™ comes with Google inception

model whereas on the other hand NVIDIA DIGITS uses alexnet caffe model and googlenet model.

6.2.1 TensorFlow™

TensorFlow™ is an open source software library for leaning numerical computation using data flow graphs. Nodes in the graph represent mathematical operations, while the graph edges represent the multidimensional data arrays (tensors) communicated between them. The flexible and reliable architecture allows its users to easily deploy numerical computation to one or more parallel computing systems which includes both CPUs and GPUs in a desktop, server, or mobile device with a single API. TensorFlow was originally developed by team of researchers and engineers working on the Google Brain Team within Google's Machine Intelligence research organization for the purposes of conducting machine learning and deep neural networks research, but the system is general enough to be applicable in a wide variety of other domains as well [67]. TensorFlow utilizes Convolution Neural Networks (CNN) to learn its classifiers. It works on Linux based plate forms which includes Ubuntu and can be compiled using python and c++ compilers. TensorFlow library comes with pre-trained Inception-v3 (GoogLeNet) model which can be retrained for the custom classification purpose.

6.2.2 NVIDIA DIGITS

NVIDIA DIGITS is another one of the state of the art deep learning library developed by NVIDIA. The NVIDIA Deep Learning GPU Training System (DIGITS) puts the power of deep learning into the hands of engineers and data scientists for precise and accurate results. DIGITS can be used to rapidly train the highly accurate deep neural network (DNNs) for image classification, segmentation and object detection tasks [50]. It comes with web based graphical user interface (GUI) which makes it much easier to use. The reliable architecture allows the users to easily deploy DIGITS library on one or more parallel graphical processing units (GPUs) in desktop and servers. NVIDIA DIGITS library is only compatible with NVIDIA CUDA® capable GPU. CUDA® is a parallel computing platform and programming model that enables dramatic increases in computing performance by harnessing the power of the graphics processing unit (GPU). Like TensorFlow library it also works on Linux based plate forms which includes Ubuntu. NVIDIA DIGITS utilizes pre-trained model which includes Alexnet caffe model which can be retrained for custom image classification purpose.

6.3 Deep Learning Models

For the proposed research work two state of the art deep neural networks are utilized which are as following

6.3.1 Inception v3 Model

The Inception v3 model is one of the best Google image classifier. It is made up of many layers stacked on top of each other [20]. Inception v3 model was trained using 1.2 million images from 1000 different categories and training of inception models took 2 weeks. These layers are pre-trained and are already very valuable at finding and summarizing information that will help classify most of the images from real world environment. Figure 6.1 shows the inception model layer architecture.

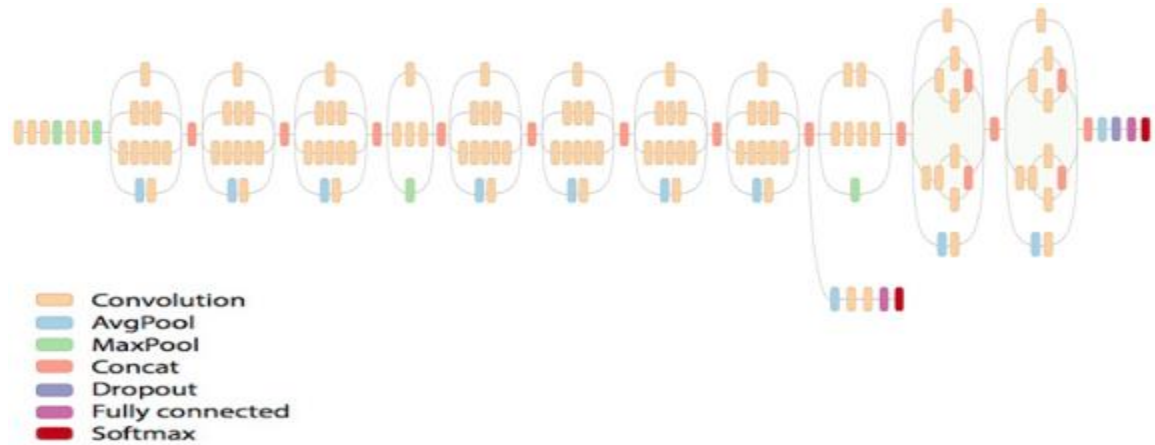


Figure 6.1: Detailed Inception model layer architecture which includes convolution layer, avgpool layers, maxpool layers, concat layers, dropout layers, fully connected and softmax layers [42]

6.3.2 Alexnet Caffe Model

Alexnet model is advanced version of Lenet model. It is also a multilayer model and it is considered as one of the best image classifier. Alexnet model is trained using a collection of 1.3 million images from 1000 different classes collected from ImageNet Library and can classify most of the images from real world environment [25]. Complete layer architecture of Alexnet model is shown in Figure 6.2.

AlexNet

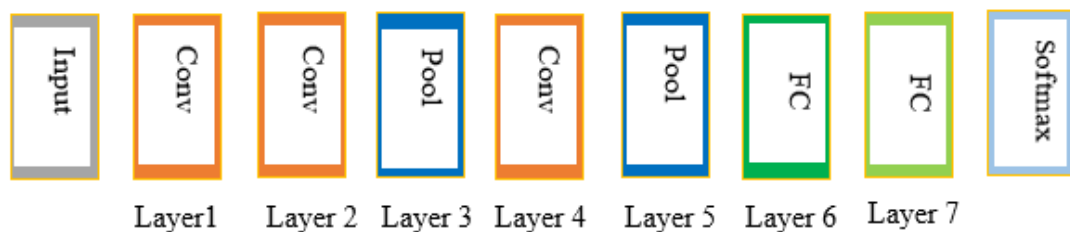


Figure 6.2: Detailed Alexnet model layer architecture which includes input layer, convolution layer, pool layers, fully connected (FC) layers and softmax layers

6.4 Hardware Requirement

The proposed deep learning libraries as discussed in section 6.2 is implemented using Linux Ubuntu 14.04 (Trusty Tahr) version and overall system is tested on HP Z440 Xeon processor machine with external NVIDIA Quadro K2200 graphic card which has 4GB of built-in memory and 128 bit of clock size. The NVIDIA Quadro K2200 is a CUDA supported GPU which has 640 CUDA Cores. The whole process of classification takes approximately up to 2 minutes and generates the final results.

6.5 TensorFlow Training and Classification Results

For the proposed skin cancer classification task we have trained the two main classes of images which included melanoma and non-melanoma images in RGB format using state of the art Google Inception V3 model. The training folder contains 200 training images collected from datasets named as tf files which is shown in [Figure 6.3](#).



Figure 6.3: Folder containing skin cancer training images categorized as melanoma and non-melanoma

For training the classifier Google Inception v3 model was used for retraining the bottleneck layers.

After storing the Google Inception v3 network the upcoming stage is preparing the datasets images which implies retraining the Inception v3 network. The Inception v3 network is a huge image classification model with millions of parameters that can differentiate between large numbers of different kinds of images [20]. For our custom classification task we will be using transfer learning method to subsequently train the Bottleneck layers. A 'Bottleneck,' is a term we often use for the layer that is just before the final output layer and actually does the classification. Thus, the overall training will end in sensible measure of time. Every image is reused multiple times during training and Bottleneck feature values will be created against each training image. It creates more than 200 Bottleneck feature values against each image which will be saved in tf files folder. The re training of Google Inception v3 is shown in [Figure 6.4](#)

```

Creating bottleneck at /tf_files/bottlenecks/melanoma/SSM13_orig.jpg.txt
Creating bottleneck at /tf_files/bottlenecks/melanoma/SSM32_orig.jpg.txt
Creating bottleneck at /tf_files/bottlenecks/melanoma/LMM4_orig.jpg.txt
Creating bottleneck at /tf_files/bottlenecks/melanoma/SSM23_orig.jpg.txt
Creating bottleneck at /tf_files/bottlenecks/melanoma/SSM70_orig.jpg.txt
Creating bottleneck at /tf_files/bottlenecks/melanoma/SSM42_2_orig.jpg.txt
Creating bottleneck at /tf_files/bottlenecks/melanoma/LMM3_orig.jpg.txt
Creating bottleneck at /tf_files/bottlenecks/melanoma/LMM11_orig.jpg.txt
Creating bottleneck at /tf_files/bottlenecks/melanoma/SSM21_orig.jpg.txt
Creating bottleneck at /tf_files/bottlenecks/melanoma/NM4_orig.jpg.txt
Creating bottleneck at /tf_files/bottlenecks/melanoma/SSM74_orig.jpg.txt
Creating bottleneck at /tf_files/bottlenecks/melanoma/LMM8_2_orig.jpg.txt
Creating bottleneck at /tf_files/bottlenecks/melanoma/SSM9_orig.jpg.txt

```

(a)

```

Creating bottleneck at /tf_files/bottlenecks/melanoma/SSM12_orig.jpg.txt
Creating bottleneck at /tf_files/bottlenecks/melanoma/SSM27_orig.jpg.txt
Creating bottleneck at /tf_files/bottlenecks/melanoma/SSM30_orig.jpg.txt
Creating bottleneck at /tf_files/bottlenecks/melanoma/LMM2_orig.jpg.txt
Creating bottleneck at /tf_files/bottlenecks/non-melanoma/26_orig.jpg.txt
Creating bottleneck at /tf_files/bottlenecks/non-melanoma/41_orig.jpg.txt
Creating bottleneck at /tf_files/bottlenecks/non-melanoma/45_orig.jpg.txt
Creating bottleneck at /tf_files/bottlenecks/non-melanoma/D45_2_orig.jpg.txt
Creating bottleneck at /tf_files/bottlenecks/non-melanoma/D53_2_orig.jpg.txt
Creating bottleneck at /tf_files/bottlenecks/non-melanoma/10_orig.jpg.txt
Creating bottleneck at /tf_files/bottlenecks/non-melanoma/D23_2_orig.jpg.txt

```

(b)

Figure 6.4: Google Inception v3 network creating bottleneck values against each image in training folder divided in to two main classes melanoma and non-melanoma in text format.

After creating the bottleneck values against each image in training folder the Inception model starts retraining itself using transfer learning methodology. The process iterates for 4000 times and generates final train accuracy of 100 % and test accuracy of 83.4 % which is shown in [Figure 6.5](#). The detailed accuracy and cross entropy graph results are shown in [Figure 6.6](#).

```

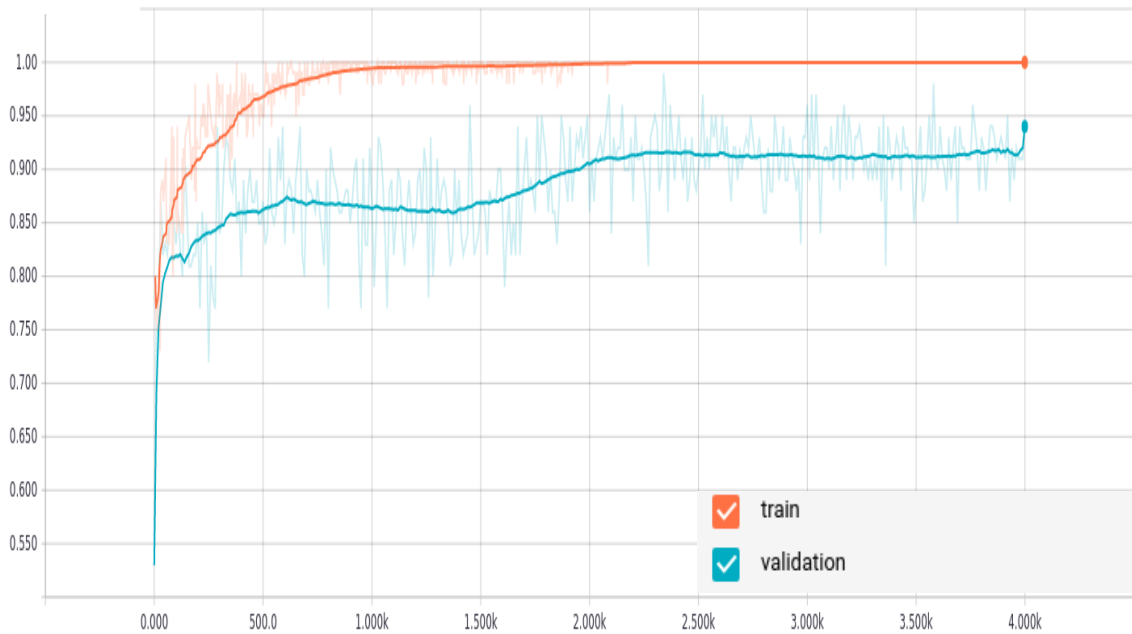
2017-02-27 05:42:02.465366: Step 3980: Train accuracy = 100.0%
2017-02-27 05:42:02.465621: Step 3980: Cross entropy = 0.033830
2017-02-27 05:42:02.564695: Step 3980: Validation accuracy = 91.0%
2017-02-27 05:42:03.138762: Step 3990: Train accuracy = 100.0%
2017-02-27 05:42:03.139019: Step 3990: Cross entropy = 0.035414
2017-02-27 05:42:03.238453: Step 3990: Validation accuracy = 91.0%
2017-02-27 05:42:03.772123: Step 3999: Train accuracy = 100.0%
2017-02-27 05:42:03.772375: Step 3999: Cross entropy = 0.033169
2017-02-27 05:42:03.872084: Step 3999: Validation accuracy = 94.0%
Final test accuracy = 83.4%
Converted 2 variables to const ops.
root@f57d77e6d84f: /tensorflow# █

```

(a)

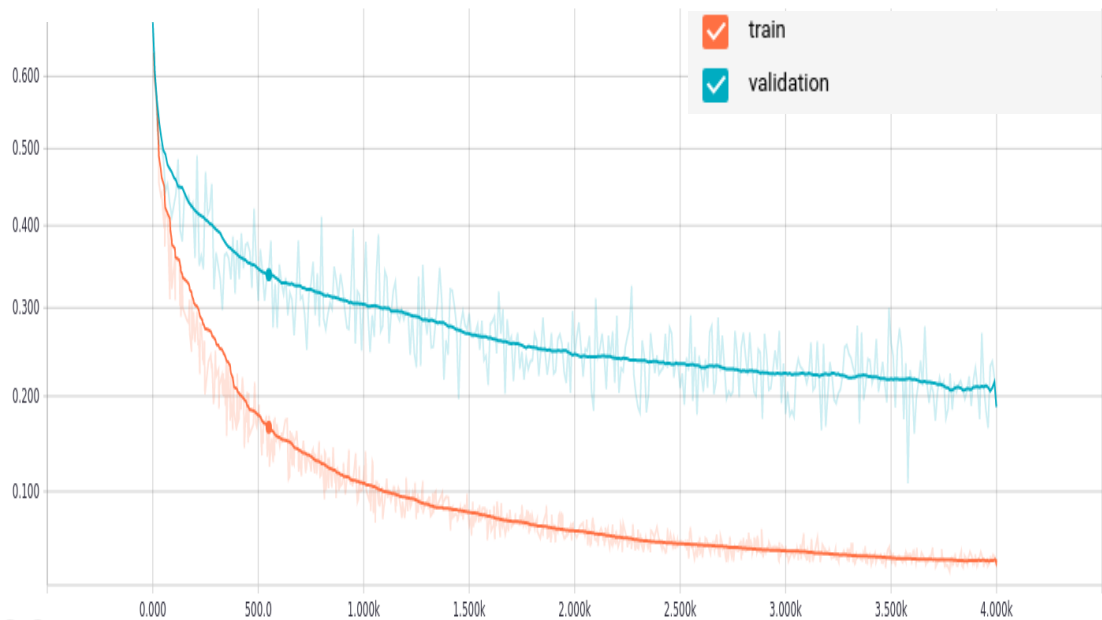
Figure 6.5: The retraining process of Google Inception v3 network with final train accuracy of 100 % and test accuracy of 83.4 %.

accuracy



(a) Accuracy graph of TensorFlow library where orange line represents the train accuracy of 90 % and blue line represents the validation accuracy of 100% for 4000 iterations.

cross entropy



(b). Overall cross entropy graph of TensorFlow library where orange line represents the train cross entropy and blue line represents the validation cross entropy for 4000 iterations.

Figure 6.6: The detailed (a) accuracy and (b) cross entropy graph of TensorFlow library for 4000 iterations.

After creating the bottleneck values against each image in training folder and retraining of Inception v3 network the next phase is to test the classifiers on certain test cases. The classification results were obtained from various test cases in RGB format. The test cases images are shown in [Figure 6.7](#).



Figure 6.7: The test case folder containing test cases images in RGB format from both melanoma and non-melanoma classes.

The classification results obtained from the test cases are shown below. The complete classification results for all the test cases are shown in [Table 6.1](#) according to which 15 cases were classified correctly when compared with ground truth whereas 2 cases were miss classified when compared with ground truth results having the accuracy of 88 %. These test cases were also classified using Artificial Neural Network (ANN) according to which 5 case were miss classified when compared with ground truth results having low accuracy level of 70.6 % as compared to TensorFlow results.

Test Case 3

The desired case is melanoma with 99.7% accuracy which are true results according to ground truths of provided dataset

```
root@f9505f79007b:~# python /tf_files/
W tensorflow/core/framework/op_def_util
. Use tf.nn.batch_normalization().
melanoma (score = 0.99772)
non melanoma (score = 0.00228)
```

Test Case 11

The desired case is non-melanoma with 96.9% accuracy which are true results according to ground truths of provided dataset

```
root@f9505f79007b:~# python /tf_files/
W tensorflow/core/framework/op_def_util
. Use tf.nn.batch_normalization().
non melanoma (score = 0.96964)
melanoma (score = 0.03036)
```

TABLE 6.1: Classification Results using TensorFlow Library

TensorFlow Classifier Results			
Test Case	Classification Results Using TensorFlow (Confidence %)	Classification Results Using ANN	Ground Truth Results
1	Non-Melanoma (88.5 %)	1 (Melanoma)	Melanoma (Risk Level: High)
2	Melanoma (98.8 %)	1 (Melanoma)	Melanoma (Risk Level: High)
3	Melanoma (99.7 %)	1 (Melanoma)	Melanoma (Risk Level: High)
4	Melanoma (99.6 %)	1 (Melanoma)	Melanoma (Risk Level: High)
5	Melanoma (99.4 %)	1 (Melanoma)	Melanoma (Risk Level: High)
6	Non-Melanoma (79.4 %)	1 (Melanoma)	Melanoma (Risk Level: High)
7	Melanoma (90.8 %)	0 (Non-Melanoma)	Melanoma (Risk Level: High)
8	Melanoma (89.9 %)	1 (Melanoma)	Melanoma (Risk Level: High)
9	Melanoma (98.7 %)	1 (Melanoma)	Melanoma (Risk Level: High)
10	Non-Melanoma (94.8 %)	1 (Melanoma)	Non-Melanoma (Risk Level: Low)
11	Non-Melanoma (96.9 %)	1 (Melanoma)	Non-Melanoma (Risk Level: Low)
12	Non-Melanoma (97.4 %)	1 (Melanoma)	Non-Melanoma (Risk Level: Low)
13	Non-Melanoma (93.3 %)	0 (Non-Melanoma)	Non-Melanoma (Risk Level: Low)
14	Non-Melanoma (97.9 %)	0 (Non-Melanoma)	Non-Melanoma (Risk Level: Low)
15	Non-Melanoma (92.2 %)	0 (Non-Melanoma)	Non-Melanoma (Risk Level: Low)
16	Non-Melanoma (99.2 %)	0 (Non-Melanoma)	Non-Melanoma (Risk Level: Low)
17	Non-Melanoma (98.9 %)	1 (Melanoma)	Non-Melanoma (Risk Level: Low)

6.6 NVIDIA DIGITS Training and Classification Results

For the proposed research work second state of the art NVIDIA DIGITS library is used for skin cancer classification task. Like TensorFlow we have trained skin cancer dataset containing two main classes of images which includes melanoma and non-melanoma images in RGB format using Caffe Alexnet model. The training dataset is shown in Fig 6.8



Figure 6.8: The skin cancer dataset in png image encoding for training the state of the art Caffe Alexnet model

After creating the skin cancer dataset folder in NVIDIA DIGITS web bases graphical user interface (GUI) system the next phase is retraining of Caffe Alexnet model which is done by creating custom classification model named as Malignancy-Measure which is shown in Figure 6.9.

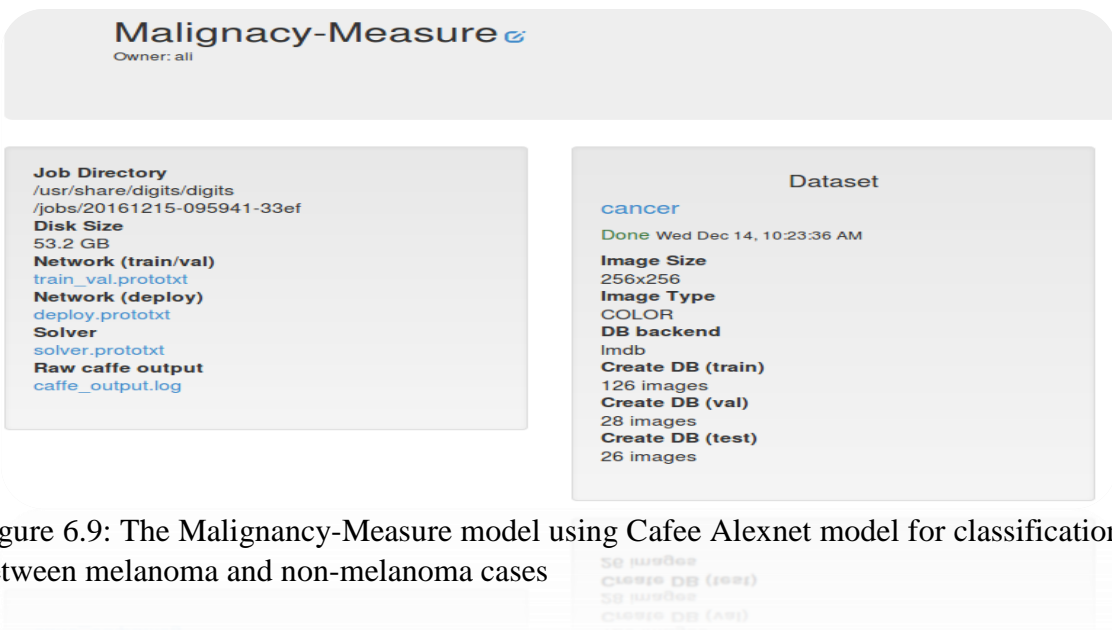


Figure 6.9: The Malignancy-Measure model using Caffe Alexnet model for classification between melanoma and non-melanoma cases

After creating the custom Malignancy-Measure model based on Caffe Alexnet model the next phase is the training of model using transfer learning methodology. The process iterates for 250 epochs and generates final train accuracy of 81 % [Figure 6.10](#).

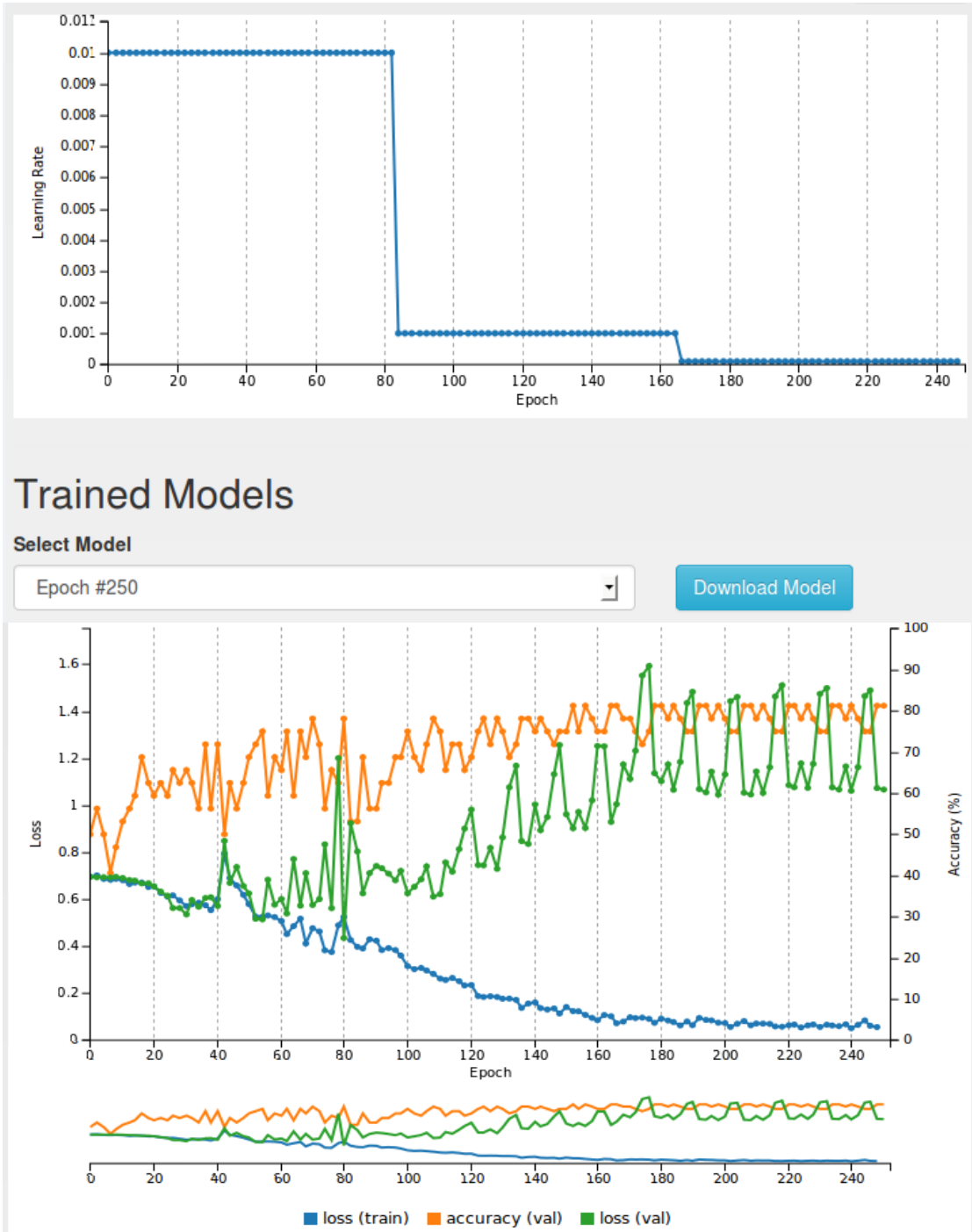


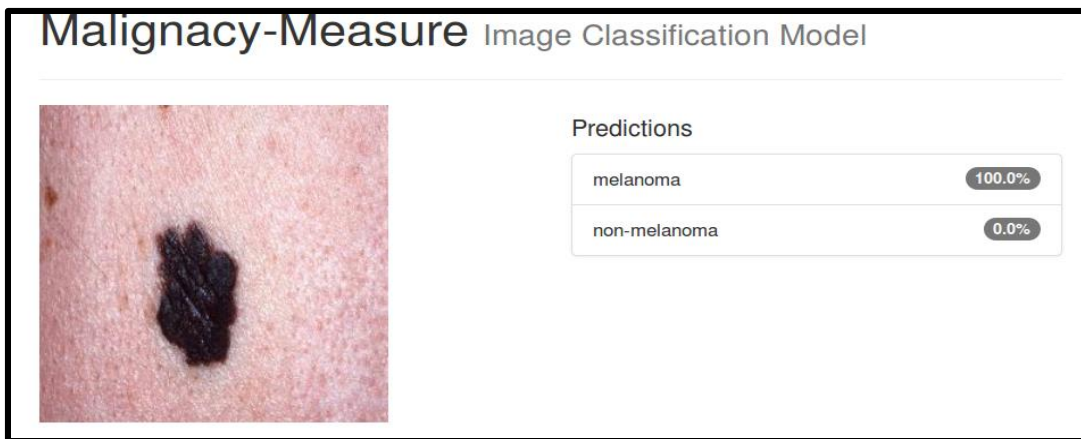
Figure 6.10: The training process of Malignancy-Measure model using Caffe Alexnet model with final train accuracy of 81% and training loss of 2%

After training Malignancy-Measure model using Caffe Alexnet model with overall training accuracy of 81% the next step is to test our classifier on certain test cases. The classification results were obtained from various test cases shown in [Figure 6.7](#).

The classification results obtained from the test cases are shown below. The overall detailed results for test case 3 is shown in [Figure 6.11](#). The complete classification results for all the test cases are shown in [Table 6.2](#) according to which 14 cases were classified correctly when compared with ground truth whereas 3 cases were miss classified when compared with ground truth results having the accuracy of 82 %. These test cases were also classified using Artificial Neural Network (ANN) according to which 5 case were miss classified when compared with ground truth results having low accuracy level of 70.6 % as compared to NVIDIA DIGITS results.

Test Case 3

The desired case is melanoma with 100 % accuracy which are true results according to ground truths of provided dataset

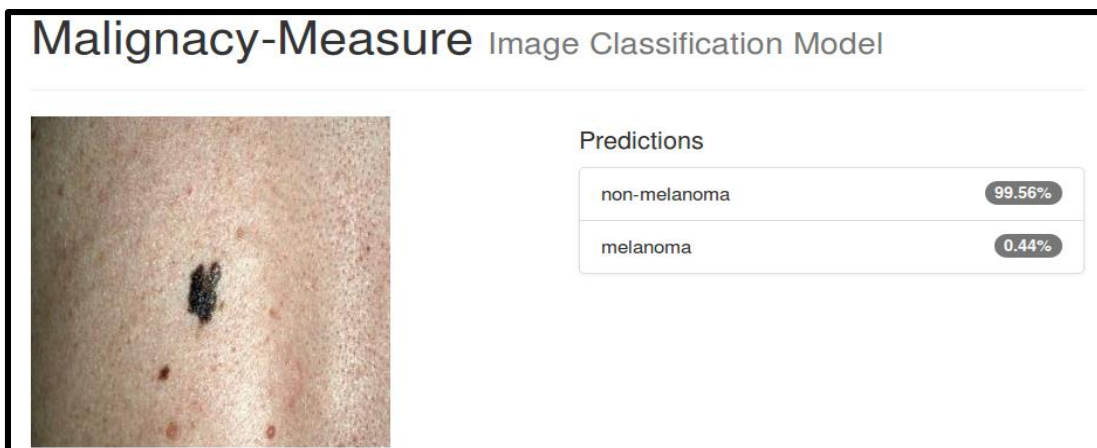


Malignancy-Measure Image Classification Model

Predictions	
melanoma	100.0%
non-melanoma	0.0%

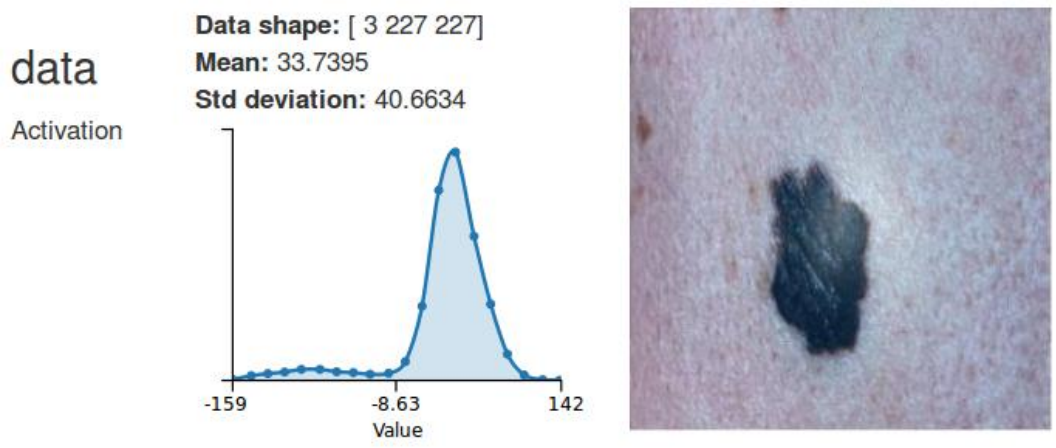
Test Case 11

The desired case is non-melanoma with 99.56 % accuracy which are true result according to ground truths of provided dataset

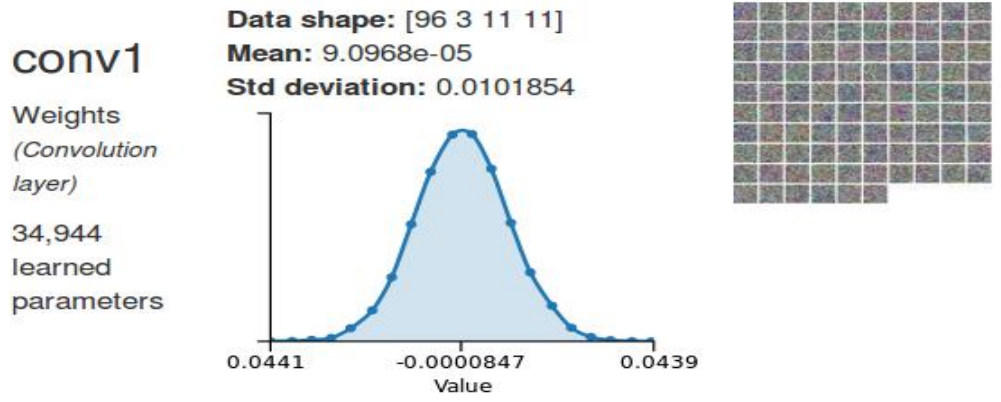


Malignancy-Measure Image Classification Model

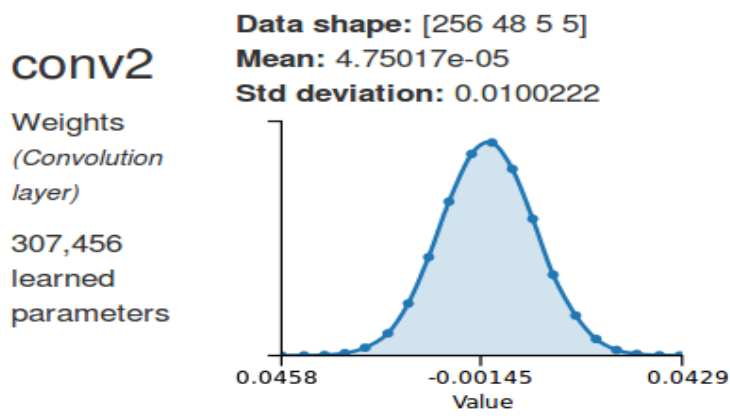
Predictions	
non-melanoma	99.56%
melanoma	0.44%



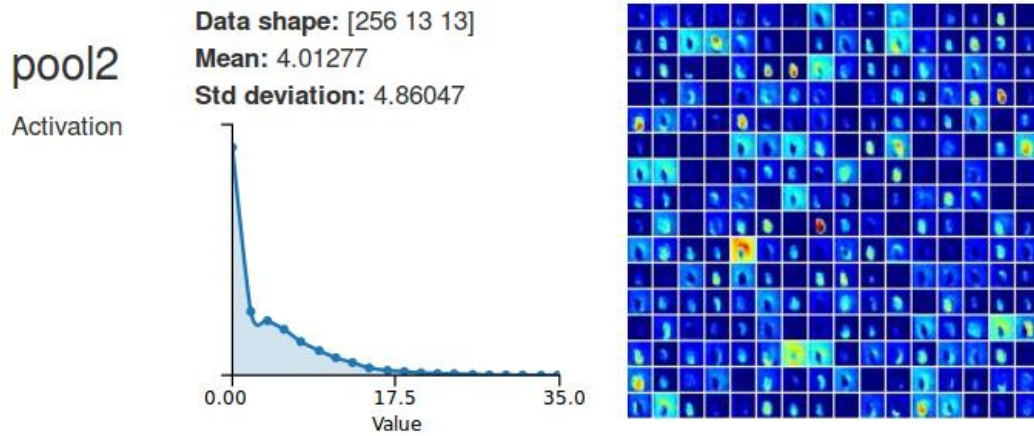
(a) Mean and Standard deviation values of desired test case



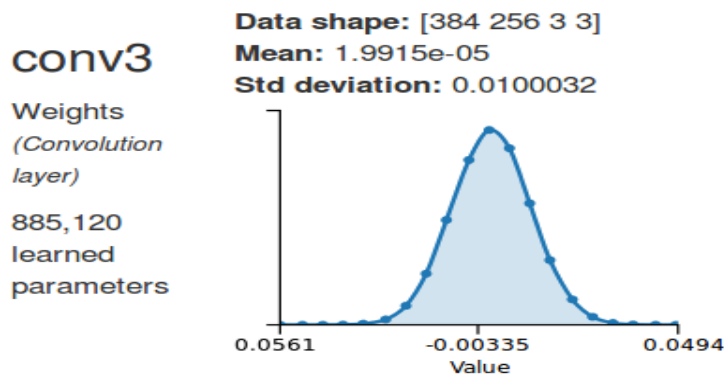
(b) Convolution 1 layers results with total 34,944 learned parameters



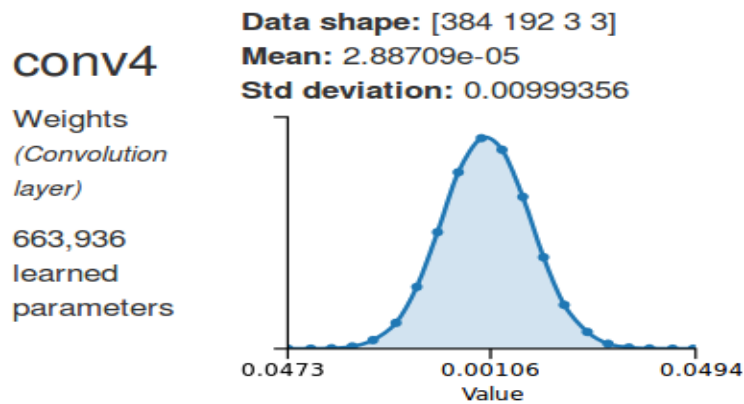
(c) Convolution 2 layers results with total 307,456 learned parameters



(d) pool 2 layers results with its mean and standard deviation value



(e) Convolution 3 layers results with total 885.120 learned parameters



(f) Convolution 3 layers results with total 663,936 learned parameters

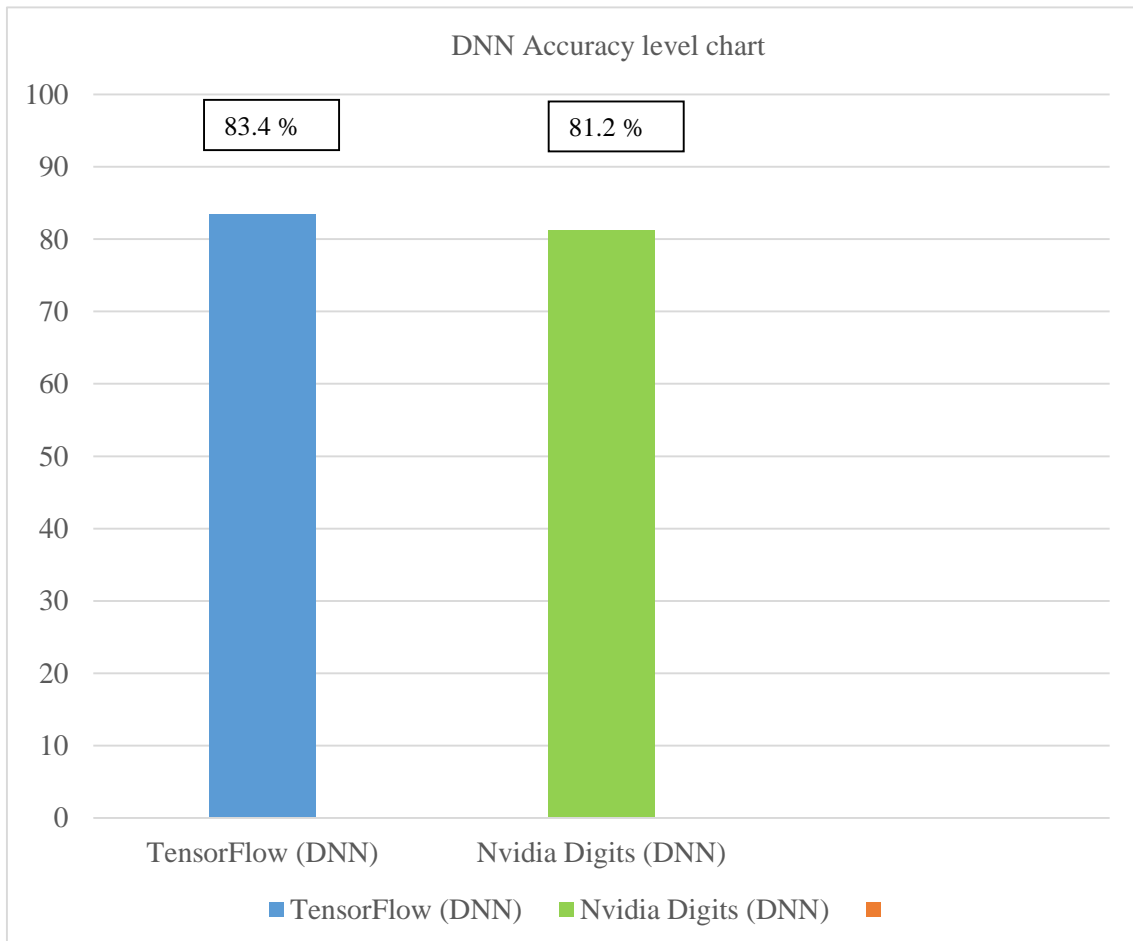
Figure 6.11: Detailed results (a), (b), (c), (d), (e) and (f) for test case 3 with statistical parameters.

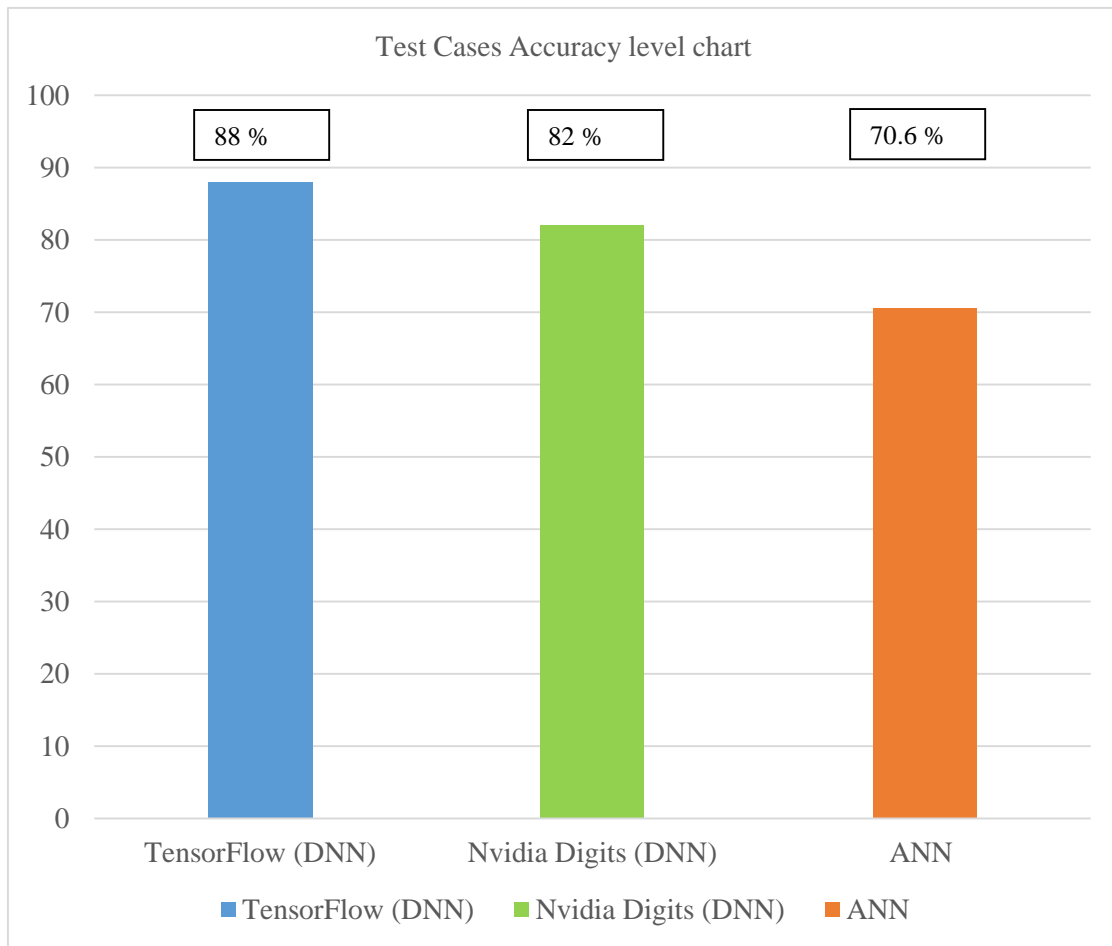
TABLE 6.2: Classification Results using NVIDIA DIGITS Library

NVIDIA DIGITS Classifier Results			
Test Case	Classification Results Using NVIDIA DIGITS (Confidence %)	Classification Results Using ANN	Ground Truth Results
1	Non-Melanoma (75.8 %)	1 (Melanoma)	Melanoma (Risk Level: High)
2	Melanoma (100 %)	1 (Melanoma)	Melanoma (Risk Level: High)
3	Melanoma (100 %)	1 (Melanoma)	Melanoma (Risk Level: High)
4	Melanoma (100 %)	1 (Melanoma)	Melanoma (Risk Level: High)
5	Melanoma (99.6 %)	1 (Melanoma)	Melanoma (Risk Level: High)
6	Melanoma (99.7 %)	1 (Melanoma)	Melanoma (Risk Level: High)
7	Non-Melanoma (88.8 %)	0 (Non-Melanoma)	Melanoma (Risk Level: High)
8	Non-Melanoma (86.1 %)	1 (Melanoma)	Melanoma (Risk Level: High)
9	Melanoma (100 %)	1 (Melanoma)	Melanoma (Risk Level: High)
10	Non-Melanoma (99.7 %)	1 (Melanoma)	Non-Melanoma (Risk Level: Low)
11	Non-Melanoma (99.5 %)	1 (Melanoma)	Non-Melanoma (Risk Level: Low)
12	Non-Melanoma (99.6 %)	1 (Melanoma)	Non-Melanoma (Risk Level: Low)
13	Non-Melanoma (98.9 %)	0 (Non-Melanoma)	Non-Melanoma (Risk Level: Low)
14	Non-Melanoma (99.7 %)	0 (Non-Melanoma)	Non-Melanoma (Risk Level: Low)
15	Non-Melanoma (99.9 %)	0 (Non-Melanoma)	Non-Melanoma (Risk Level: Low)
16	Non-Melanoma (99.7 %)	0 (Non-Melanoma)	Non-Melanoma (Risk Level: Low)
17	Non-Melanoma (99.8 %)	1 (Melanoma)	Non-Melanoma (Risk Level: Low)

6.7 Comparison Chart between DNN and ANN

The below chart shows the comparison for accuracy level between Deep Neural Network (DNN) frameworks which includes TensorFlow and NVIDIA DIGITS. The overall accuracy level of TensorFlow is 83.4 % and Nvidia Digits is 81.2 %. Moreover, the collected feature values of Deep Neural Networks are much greater as compared to conventional neural classifiers. Thus, we conclude that performance level of Deep Neural Networks is more efficient due repetitive blocks of neurons in complex mathematical structure adjusted in its multilayer hidden layer architecture. The Second chart represents the test cases accuracy shown in Table 6.1 and Table 6.2 respectively. For Artificial Neural Networks (ANN) the achieved test cases accuracy level for 17 different test cases is 70.6 % with 12 correct predictions whereas for TensorFlow the test cases accuracy level for 17 different cases is 88 % and that for NVIDIA DIGITS is 82 % which clearly reflects the improved accuracy level as compared to conventional neural classifiers.





6.8 Advantages of Deep Neural Networks (DNN)

Following are some of the advantages of the deep neural networks

- Reduces the requirement for feature extraction which is assumed as one of the most time-consuming phase in the machine learning.
- Its flexible architecture can be used to solve new issues generally with effective and robust results which is difficult to obtain using conventional classifiers.
- Collect huge amount of hidden features which is utilized for precise and accurate classification in complex domains like medical imaging.

Chapter 7

Conclusion

The overall thesis proposes three significant approaches that can be used in future computer-aided skin lesion diagnosis from dermoscopy images which includes novel merged approach for skin lesion segmentation, parallel classifiers systems and advanced deep learning methodologies for skin cancer classification.

7.1 Merged Approach for Skin Lesion Segmentation

The contribution described in this section are published in IEEE BIBE 16th International conference held in Taiwan. [10]. As computer vision research student my goal was to design the robust Automatic Lesion Detection System (ALDS) system for precise and accurate classification of skin cancer. Automatic Lesion Detection System (ALDS) for skin cancer classification is the extended work of Chang et al. [3]. Initially sharpening filter is applied and also hair removal is performed using dull razor software [14] that eventually produces more refined results. Active contours and watershed approaches are used to segment out the cancerous area automatically from the dataset image with increased efficiency. The proposed research work concludes that merged approach of watershed and active contour produces better segmented output, as compared with the individual performance of these techniques

7.2 Parallel Classifier System

The contribution described in this section are published in IEEE BIBE 16th International conference held in Taiwan [10]. The classification of cancer mole using SVM was practiced using research findings of Chang et al [3]. On the other hand ANN classifier is implemented as second level classifier to witness the results obtained from SVM and also to check the cases where SVM fails to classify. i.e. indeterminate cases. The proposed research work concludes that SVM and ANN complement each other and help to provides better classification decisions.

7.3 Deep Learning Methodologies for Skin Cancer Classification

This section describes the use of deep learning techniques for more precise and accurate classification between (non-melanoma) and cancerous (melanoma) cases as compared to conventional classifiers. My contribution includes the use of two state of art deep learning libraries which include TensorFlow and NVIDIA DIGITS for skin cancer classification with increased accuracy levels in overall classification results.

7.4 Future Work

Due to fewer number of free available datasets and number of image samples (in controlled environment) with subsequent medical diagnosis, there are certain aspects which cannot be tested at this stage and needs further analysis as future work. These include more than one cancerous mole in an image, varying illumination conditions and slightly varying pose of the region of interest. Moreover, classification between non melanoma skin cancers like Basal Cell Carcinoma (BCC) and Squamous Cell Carcinoma (SCC) is also included in the future challenges. These factors are expected to change the features characteristics and is an open problem to research community. Moreover, the accuracy of neural networks and deep neural networks (DNN) can also be further enhanced by increasing the number of samples and the number of features in the training phase. Additionally, in future this system can be made to learn the evolution of the cancerous mole before time based on probabilistic and forecasting measures. This will require test images of the same case progressing over time.

Bibliography

- [1] Amir A. Amini, Terry A. Weymouth and Ramesh C. Jain, "Using Dynamic Programming for Solving Variation Problems in Vision", Published in *IEEE Transactions on Pattern Analysis and Machine Intelligence*, Volume 12(9), pp. 855-867, September, 1990.
- [2] Bleau AL, Leon LJ. Watershed-based segmentation and region merging. *Computer Vis Image Underst.* 2000;77:317–370.
- [3] Chang Wen-Yu, Adam Huang, Chung-Yi Yang, Chien-Hung Lee, Yin-Chun Chen, Tian-Yau Wu and Gwo-Shing Chen, "Computer-Aided Diagnosis of Skin Lesions Using Conventional Digital Photography: A Reliability and Feasibility Study", Published in *PLoS ONE*, Volume 8(11), e76212, November 2013
- [4] Chen X. PhD dissertation. Department of Electrical and Computer Engineering, University of Missouri-Rolla; 2007. Skin lesion segmentation by an adaptive watershed flooding approach segmentation by an adaptive watershed flooding approach.
- [5] D.J. Gawkrödger. "Dermatology: an illustrated colour text" published in. *Elsevier Health Sciences*, 2002.
- [6] Derraz, Foued M. Beladgham, M. Khelif, "Application of active contour models in medical image segmentation", Published in IEEE international Conference on *Information Technology: Coding and Computing, Proceedings. ITCC volume 2*, 5-7 April 2004.
- [7] Doi, Kunio. "Computer-aided diagnosis in medical imaging: historical review, current status and future potential." Published in *Computerized medical imaging and graphics 31.4 (2007): 198-211*, 2007
- [8] El Allaoui Ahmed and M'barek Nasri "Medical Image Segmentation By Markercontrolled Watershed and Mathematical Morphology" Published in the *International Journal of Multimedia & Its Applications (IJMA) Vol.4, No.3*, June 2012
- [9] Farag, Aly A., et al. "Advanced segmentation techniques." *Handbook of biomedical image analysis*. Springer US, 2005. 479-533.
- [10] Farooq Muhammad Ali, Muhammad Aatif Mobeen Azhar, and Rana Hammad Raza. "Automatic Lesion Detection System (ALDS) for Skin Cancer Classification Using SVM and Neural Classifiers." Published in *Bioinformatics and Bioengineering (BIBE), 2016 IEEE 16th International Conference on*. IEEE, 2016,
- [11] Garnavi Rahil, Mohammad Aldeen and James Bailey, "Computer- Aided Diagnosis of Melanoma Using Border and Wavelet-based Texture Analysis", Published in IEEE *Trans Inf Technol Biomed*, Volume 16(6), pp. 1239-52, November, 2012.
- [12] Human Anatomy detailed layer structures, Authors: Y. Chudnovsky, P.A. Khavari, and A.E. Adams. "Melanoma genetics and the development of rational therapeutics" *Published in. Journal of Clinical Investigation*, 115.4 (2005): 813-824., 2005.
- [13] Jafari, M. H., et al. "Set of descriptors for skin cancer diagnosis using non-dermoscopic color images." *Image Processing (ICIP), 2016 IEEE International Conference on*. IEEE, 2016.
- [14] Lee T, Ng V, Gallagher R, Coldman A, McLean D. DullRazor: "A software approach to hair removal from images" Published in the *Computers in Biology and Medicine*, 1997

- [15] Mendonça Teresa, Pedro M. Ferreira, Jorge Marques, Andre R. S. Marcal, Jorge Rozeira, “PH² - A dermoscopic image database for research and benchmarking”, Published in the Proceedings of *35th International Conference of the IEEE Engineering in Medicine and Biology Society*, July 3-7, 2013.
- [16] Petrick N1, Sahiner B, Armato SG 3rd, Bert A, Correale L, Delsanto S “Evaluation of computer-aided detection and diagnosis systems”, Published in *The International Journal of Medical Physics Research and Practice*, August 1, 2013.
- [17] Ray, Pravda Jith, S. Priya, and T. Ashok Kumar. "Nuclear segmentation for skin cancer diagnosis from histopathological images." *Communication Technologies (GCCT), 2015 Global Conference on*, IEEE, 2015.
- [18] Rigel, Darrell S., Julie Russak, and Robert Friedman. "The evolution of melanoma diagnosis: 25 years beyond the ABCDs." *CA: a cancer journal for clinicians* 60.5 (2010): 301-316.
- [19] Sujitha, S., et al. "A combined segmentation approach for melanoma skin cancer diagnosis." Published in *Computing, Communication and Information Systems (NCCCIS), 2015 IEEE Seventh National Conference on*. IEEE, 2015
- [20] Szegedy, Christian, et al. "Going deeper with convolutions." Published in Proceedings of the *IEEE Conference on Computer Vision and Pattern Recognition*. 2015
- [21] Vincent L, Soille P. “Watersheds in digital spaces: an efficient algorithm based on immersion simulations”, Published in *IEEE Transactions on Pattern Analysis and Machine Intelligence Volume 13*, 1991
- [22] Yuan, Xiaojing, et al. "SVM-based texture classification and application to early melanoma detection." *Engineering in Medicine and Biology Society, 2006. EMBS'06. 28th Annual International Conference of the IEEE*. IEEE, 2006.
- [23] Yun Tian ; Coll. of Inf. Sci. & Technol., BNU, Beijing, China; Ming-quan Zhou; Zhong-ke Wu Xing-ce Wang “A Region-Based Active Contour Model for Image Segmentation “ Published in *IEEE Transactions on Computational Intelligence and Security, 2009. CIS '09. International Conference on (Volume: 1) pp. 376 – 380*, Dec 2009.
- [24] Basal Cell Carcinoma, Web Link: <https://www.dermnetnz.org/topics/basal-cell-carcinoma>, (Last accessed on 15 Dec 2016)
- [25] Caffe Alexnet Model, Web Link <http://www.hirokatsukataoka.net/research/cnnfeatureevaluation/cnnfeatureevaluation.html>, (Last Accessed on: 17th Dec.2016)
- [26] Caffe Barkley Vision Library, Web Link: <http://caffe.berkeleyvision.org>, (Last accessed on 29th Dec 2016).
- [27] Cancer Research UK, Web Link: <http://www.cancerresearchuk.org/health-professional/cancer-statistics/statistics-by-cancer-type/skin-cancer/incidence#heading-Five>, (Last accessed on 10th Dec 2016)
- [28] Clinical Diagnosis Technique ABCDE Method, Web Link: <https://www.melanoma.org/understand-melanoma/diagnosing-melanoma/detection-screening/abcdes-melanoma>, (Last accessed on 18th Dec.2016)
- [29] Clinical Diagnosis Technique CASH Method, Web Link: <http://www.dermnetnz.org/cme/dermoscopy-course/other-algorithms-for-melanocytic-lesions/>, (Last accessed on 11th Dec 2016)

- [30] Clinical Diagnosis Technique Menzies Method, Web Link: <http://www.mmmp.org/MMMP/import.mmmp?page=dermoscopy.mmmp>, (Last accessed on 25 Dec 2016)
- [31] Clinical Diagnosis Technique Seven Point Check List Method, Web Link: <https://www.ncbi.nlm.nih.gov/pmc/articles/PMC3635581/>, (Last accessed on 13th Dec 2016)
- [32] Data Set 01 Web Link: PH² Database, <http://www.fc.up.pt/addi/ph2%20database.html>, (Last Accessed on: 11th Jun., 2016)
- [33] Data Set 02 Web Link: Dermatology Information System, <http://www.dermis.net>, 2012. (Last Accessed on: 11th Jun., 2016)
- [34] Data Set 03 Web Link: DermQuest, <http://www.dermquest.com>, 2012. (Last Accessed on: 11th Jun., 2016).
- [35] Deep Neural Networks, Author Michael A Nielsen, “Neural Network and Deep Learning”, Determination Press, 2015, Web Link: <http://neuralnetworksanddeeplearning.com/chap5.html>, (Last accessed on 1st Jan 2017)
- [36] Dermofit Image Library, Web Link: <https://licensing.eri.ed.ac.uk/i/software/dermofit-image-library.html>, , (Last accessed on 10th Dec 2016).
- [37] Dermoscopic Image Results, Web Link: <http://www.actasdermo.org/en/diagnostic-utility-dermoscopy-in-pigmented/articulo/S1578219011000588>, (Last accessed on 29th Dec 2016)
- [38] Dermoscopic Images, Web Link: <http://www.dermoscopy.org/>, (Last accessed on 14 Dec 2016)
- [39] Extensive classification between the normal and melanoma mole utilizing ABCDE clinical diagnosis method for skin tumor classification, Web Link: <http://www.artaderm.com/skin-cancer/>, (Last accessed on 25th Dec 2016)
- [40] Human Skin Layers Hypodermis, Web Link: <http://www.sharecare.com/healthy-skin/what-is-subcutaneous-tissue>, (Last accessed on 22 Dec 2016)
- [41] Human Skin Layers, Web Link: <https://www.britannica.com/science/human-skin>, (Last accessed on 1st Jan 2017)
- [42] Inception model Layer Architecture and Retraining Inception V3 model in TensorFlow, WebLink: <https://research.googleblog.com/2016/03/train-your-own-image-classifier-with.html>, (Last Accessed on: 11th Dec., 2016)
- [43] Jaccard Similarity Coefficient. Web Link: <http://ag.arizona.edu/classes/rnr555/lecnotes/10.html> (Last Accessed on: 11th Jun., 2016).
- [44] MatConvnet Deep Learning Library, Web Link: <http://www.vlfeat.org/matconvnet>, (Last accessed on 29th Dec 2016).
- [45] MelaFind CAD System, Web Link : <http://www.fda.gov/MedicalDevices/ProductsandMedicalProcedures/DeviceApprovalsandClearances/Recently-ApprovedDevices/ucm280864.htm>, (Last accessed on 24th Dec 2016)
- [46] Melanoma Risk Factors, Web Link: <http://www.mayoclinic.org/diseases-conditions/melanoma/basics/definition/con-20026009>, (Last accessed on 15 Dec 2016)
- [47] Melanoma Skin Cancer, Web Link: <http://www.mayoclinic.org/diseases-conditions/melanoma/multimedia/melanoma/img-20006924>, (Last accessed on 16 Dec 2016)

- [48] Mole Max CAD System, Web Link: <http://www.skinhealthclinic.melbourne/prices>, (Last accessed on 26th Nov 2016)
- [49] Neural Network Interconnected layer Network, Author Michael A Nielsen, “Neural Network and Deep Learning”, Determination Press, 2015, Web Link: <http://neuralnetworksanddeeplearning.com/chap5.html> (Last accessed on 20 Dec 2016)
- [50] NVIDIA Digits Deep Learning Library, Web Link: <https://developer.nvidia.com/digits>, (Last accessed on 29th Dec 2016).
- [51] Organs of the Body, Web Link: <http://hubpages.com/education/Human-Skin-The-largest-organ-of-the-Integumentary-System>, (Last accessed on 22 Dec 2016)
- [52] Prevention from Skin Cancer Web Link:<http://www.skincancer.org/prevention/sun-protection/prevention-guidelines>, (Last accessed on 2nd Dec 2016)
- [53] Region Based Segmentation Techniques, ,Web Link: <http://www.doc.ic.ac.uk/~dfg/vision/v02.html>, (Last accessed on 18th Dec 2016)
- [54] Skin Cancer Facts and Figures in Growing Ages, Web Link: <https://www.aimatmelanoma.org/about-melanoma/melanoma-stats-facts-and-figures/>, (Last accessed on 10th Dec 2016)
- [55] Skin Cancer Facts and Figures, Web Link: <http://www.skincancer.org/skin-cancer-information/skin-cancer-facts>, (Last accessed on 29th Dec 2016)
- [56] Skin Cancer Facts in Growing Ages, Web Link: <http://webcache.googleusercontent.com/search?q=cache:http://www.skincancer.org/skin-cancer-information/skin-cancer-facts>, (Last accessed on 18 Dec 2016)
- [57] Skin Cancer Risk Factors. Web Link: <http://www.cancer.org/cancer/skincancer-melanoma/detailedguide/melanoma-skin-cancer-risk-factors>, (Last Accessed on: 11th Jun., 2016).
- [58] Skin Cancer Treatments, Web Link: [http://www.skincancer.org/skin-cancer-information/squamous-cell-carcinoma/scc-treatment options](http://www.skincancer.org/skin-cancer-information/squamous-cell-carcinoma/scc-treatment-options), (Last accessed on)
- [59] Solar Scan CAD System, Web Link: <http://www.eyramedical.com.au/solar-scan-skin-cancer.shtml>, (Last accessed on 25th Nov 2016)
- [60] Sorenson Dice Similarity Coefficient. Web link: <https://brenocon.com/blog/2012/04/f-scores-dice-and-jaccard-set-similarity/> (Last Accessed on: 11th Jun. 2016).
- [61] Squamous Cell Carcinoma Sample Case, Web Link: <http://www.illinoisderm.com/services/squamous-cell-carcinoma/>, (Last accessed on 14 Dec 2016)
- [62] Squamous Cell Carcinoma, Web Link: <http://www.skincancer.org/skin-cancer-information/squamous-cell-carcinoma>, (Last accessed on 15 Dec 2016)
- [63] State of the Art Classifiers, Web Link: <http://homepages.inf.ed.ac.uk/rbf/HIPR2/classify.htm>, (Last accessed on 26th Dec 2016)
- [64] Structural Similarity Index. Web Link: <http://www.mathworks.com/help/images/ref/ssim.html> (Last Accessed on: 11th Jun., 2016).
- [65] Support Vector Machines Classification Process, Web Link: <https://www.analyticsvidhya.com/blog/2015/10/understaing-support-vector-machine-example-code>, (Last accessed on 26 Dec 2016)

- [66] Support Vector Machines for Non Linear Classification Process, Web Link: <http://people.revoledu.com/kardi/tutorial/SVM/What-is-SVM-An-intuitive-introduction.html> introduction.html, (Last accessed on 26th Dec 2016)
- [67] TensorFlow Deep Learning Library, Web Link: <https://www.tensorflow.org/>, (Last accessed on 29th Dec 2016).
- [68] Theano Deep Learning Library, Web Link: <http://deeplearning.net/software/theano/> , (Last accessed on 29th Dec 2016).
- [69] Types of Skin Moles , Web Link: <https://skinvision.com/en/articles/types-of-skin-moles-and-how-to-know-if-they-re-safe>, (Last accessed on on 22 Dec 2016)
- [70] Watershed Segmentation issues, Web Link: <https://svi.nl/watershed>, (Last accessed on 11 Dec 2016)
- [71] Watershed Segmentation Technique Web Link: www.imagemet.com/WebHelp6/Default.htm#PnPMethods/Watershed_Segmentation.htm, (Last accessed on 17 Dec 2016)
- [72] Commercial Analog Dermoscopic products Web Link: www.dermlite.com/, www.dermoscan.de (Last accessed on 22 February Dec 2017)